Journal of Great Lakes Research 40 Supplement 3 (2014) 88–101

Contents lists available at ScienceDirect

Journal of Great Lakes Research

journal homepage: www.elsevier.com/locate/jglr

A Bayesian methodological framework for setting fish tumor occurrence delisting criteria: A case study in St. Marys River area of concern

Maryam Mahmood [a], E. Agnes Blukacz-Richards [a,c], Paul C. Baumann [b], Mark McMaster [c], Monir Hossain [a], George B. Arhonditsis [a,*]

[a] Ecological Modelling Laboratory, Department of Physical and Environmental Sciences, University of Toronto, Toronto, Ontario, Canada, M1C 1A4
[b] U.S. Geological Survey Columbus, OH 43229-1111, USA
[c] Environment Canada, 867 Lakeshore Road, Burlington, Ontario, Canada, L7R 4A6

ARTICLE INFO

Article history:
Received 9 September 2013
Accepted 14 February 2014
Available online 10 May 2014

Communicated by Gurbir Perhar

Index words:
Fish tumors
Bayesian inference
Delisting criteria
St. Marys River
Areas of Concern

ABSTRACT

Fish tumors and other deformities are a class of Beneficial Use Impairment (BUIs) established by the International Joint Commission to identify Areas of Concern (AOC) in the Great Lakes basin. The St. Marys River has been impaired by fish tumors and other deformities since its designation as an AOC in 1987. In this study, we present a Bayesian modeling framework that is founded upon the explicit consideration of the sampling bias in tumor observations as well as the causal association between important covariates and tumor occurrence. Data from 2009 indicate that fish tumor incidence rates were generally elevated at the Bellevue Marina and Partridge Point exposed locations relative to the Batchawana Bay reference site. Fish age was the single most important covariate of the tumor incidence rates, followed by the fork length, and the liver or gonad weights. Using the Bayesian counterpart of the two one-side tests for equivalence, the exposed site was practically equivalent to the reference location in regards to the neoplasm and pre-neoplasm incidence rates. However, the mean probability of neoplasm incidence was predicted to be lower than 10% in 70% and 95% of the cases in the exposed and reference sites, respectively. The predicted mean pre-neoplasm frequency never fell below 10% in all the samples collected at the exposed site, whereas ≈40% of the cases are predicted to fall below the proposed cut-off level in the reference site suggesting that the exposed site may still be impaired.

Introduction

Fish communities have historically been used as sentinels of change within aquatic systems due to their capacity to integrate both natural and anthropogenic stressors (Hodson et al., 1996; Iwanowicz et al., 2012; Johnson et al., 2007; van der Oost et al., 2003). In particular, tumors that arise in fish are useful indicators of environmental contamination in both freshwater and marine environments (Baumann et al., 1996; Pinkney et al., 2001, 2004). For example, polycyclic aromatic hydrocarbons (PAHs) in sediments have been connected with the development of liver cancer in brown bullhead (Baumann et al., 1996; Blazer et al., 2009a; Vogelbein et al., 1990). Numerous studies have shown an association between contaminated sediments in the Great Lakes and hepatic (liver) neoplasms in this bottom-dwelling species (Baumann and Harshbarger, 1995, 1998; Pinkney et al., 2004). Tumor prevalence surveys have been recommended for monitoring contaminated sites (Pinkney et al., 2001). Considerable discussion now revolves around refining the methodological procedures associated with fish neoplasm sampling and histopathology in order to ensure sound comparisons between impacted and unimpacted sites.

Neoplasms are generally defined as "abnormal" tissue masses that exhibit excessive, sustained growth as compared to "normal" tissues (Willis, 1952). In a Great Lakes Areas of Concern Conference (2003) related to fish tumors, they were defined as being "heritably altered…independent, relatively atypical tissue growths," which could be virally, genetically or chemically induced (Rafferty, 2003a). In a talk at the same conference, Dr. John Harshbarger outlined the difference between benign tumors (often just expanding) and cancerous tumors ("invading and destroying host tissue"), but he underscored the need for vigilance for both tumor forms, as cancers may also arise from the former ones (Rafferty, 2003a). When examining neoplasms in the context of environmental contamination in the Great Lakes area, brown bullhead (*Ameiurus nebulosus*) and white sucker (*Catostomus commersonii*) are frequently used as indicator species due to their benthic habitat and wide home range (Rafferty, 2003a). In brown bullhead, the most common neoplasms associated with environmental degradation are liver tumors (Rafferty et al., 2009), including: i) hepatocellular adenoma (benign hepatic neoplasm) and carcinoma (malignant/invasive hepatic neoplasm), and ii) bile duct neoplasms, including cholangiomas (benign) and cholangiocarcinomas (malignant). White suckers also exhibit

* Corresponding author. Tel.: +1 416 208 4858.
E-mail address: georgea@utsc.utoronto.ca (G.B. Arhonditsis).

http://dx.doi.org/10.1016/j.jglr.2014.04.003
0380-1330/

the same tumors, although they are experienced in different proportions and the histological procedures are slightly different (Hayes et al., 1990). There is also considerable research focused on the role of covariates, such as age and gender, in influencing the prevalence of neoplasms in affected fish species, with substantial evidence indicating that liver tumor prevalence increases with the age of fish (Baumann, 1992; Baumann et al., 1996; Pinkney et al., 2004).

Given the established links between hepatic neoplasms and contaminated sediments, and consequently the usefulness of tumors as indicators of environmental integrity, "fish tumors and other deformities" has been used as one of the 14 Beneficial Use Impairments set forth under the binational Great Lakes Water Quality Agreement (GLWQA). Beneficial Use Impairments (BUIs) designate areas where human activities have severely degraded water quality and ecosystem health, known as Areas of Concern (AOC). "Fish tumors and other deformities" was listed as a BUI in the 1987 amendment of the agreement due to the high prevalence of tumors in Great Lakes fish (Rafferty et al., 2009), which reached levels of 25% in certain Great Lakes regions (Baumann et al., 1996). This BUI is classified as impaired when the incidence rate of fish tumors or other deformities exceeds rates at unimpacted (control or reference) sites, or when survey data confirm the presence of neoplastic or preneoplastic liver tumors in bullhead or suckers (Rafferty et al., 2009). However, the GLWQA does not define what unimpacted sites are, what preneoplastic liver tumors are, or how rates are to be determined, causing much confusion about the specific requirements of the AOC delisting criteria. Currently, there are 14 AOCs in which the fish tumors and other deformities constitute a BUI, with only the Black River (Ohio) reclassified from impaired to "in recovery" phase and the Presque Isle Bay AOC recently taken off the list.

One of these 14 AOCs is the binational St. Marys River, a 112-km waterway that flows from Lake Superior into Lake Huron, forming an integral part of the Great Lakes-St. Lawrence Seaway. Despite being relatively less impacted compared to the Niagara River and St. Clair/Detroit River regions, due to its more remote location (Moerke and Werner, 2011), it was designated as an AOC reflecting a variety of anthropogenic impacts that have undermined the system functioning. The fish tumors and other deformities BUI was initially listed as impaired for the River due to incidences of hepatic cancers in white suckers and brown bullheads (FPS, 2010). Early surveys showed liver tumors in white suckers below the power dam in the River, as well as in brown bullheads sampled from Munuscong Bay, Michigan (EC/OMOE, 2011). The remedial action plan for the St. Marys River AOC includes management actions to address this BUI, such as improving effluent quality through the addition of secondary treatment at Essar Steel Algoma Inc. and St. Marys Paper (EC/OMOE, 2011). However, certain monitoring actions have yet to be implemented, including the comparisons of white sucker neoplasm prevalence to reference sites and revision of delisting criteria to articulate "measurable targets." As proposed now, the Fish Tumor BUI delisting criteria stipulates that this beneficial use will no longer be impaired when a survey of a locally abundant member of the sucker family, encompassing a diverse age range, indicates a liver tumor prevalence rate of less than 5% – or – a rate that is not significantly different from that of a suitable reference site.

In this paper, given the current dialogue about refining delisting criteria, the emerging knowledge about the role of fish covariates such as age, and the growing awareness about the need for probabilistic management frameworks as opposed to strictly deterministic ones (Borsuk et al., 2002; Reckhow et al., 2005), we propose a Bayesian methodological framework that incorporates these concerns and provides a possible aid for policy decisions. The purpose of our project is to develop a series of Bayesian statistical models that can be used to predict liver neoplasm and pre-neoplasm occurrence in white sucker in the St. Marys River AOC. We present three statistical formulations, Bernoulli, Zero-Inflated Poisson, and Binomial–Poisson, founded upon the causal linkages between the demographics/physical characteristics of the fish samples (e.g., age, fork length, liver/gonad weight, and total fish weight) and the likelihood of tumor incidence. In addition, the latter two models explicitly consider the impact that the sampling frequency may have on our capacity to quantify the tumor incidence rates in the system. The difference between the two models lies in the introduction of a latent variable, "true" fish tumor counts, with the Binomial–Poisson model, which is used to parameterize the causal relationship between the expected tumor incidence rates and the important covariates instead of directly employing the observed data, as the Zero-Inflated Poisson model does. We believe that these models provide a rigorous framework to evaluate fish tumor probabilities and may play an instrumental role in guiding the formation of delisting criteria across all AOCs in the Great Lakes.

Methods

Study site–data set description

The St. Marys River is a binational waterway that connects Lakes Superior and Huron (EC/OMOE, 2011). The river contains locks that facilitate ship navigation between the two lakes and flow control mechanisms and has significant economic importance for both Canada and the United States through fisheries, tourism, electricity production, steel manufacturing, and shipping (Moerke and Werner, 2011). The two major cities nearby are the twin cities of Sault Ste. Marie, Michigan (~15,000 people) and Sault Ste. Marie, Ontario (~81,000 people) (IJC, 1998). From an ecological perspective, the river and surrounding watershed/wetlands provide valuable habitats for fish and wildlife species, where some of the highest biodiversity levels in the Great Lakes basin are recorded (EC/OMOE, 2011; Moerke and Werner, 2011). In the past, the main industries in Sault Ste. Marie, ON are steel and paper manufacturing as well as other light manufacturing that generally support the two main economic activities (St. Marys River RAP, 1992). These industrial dischargers have posed serious contamination problems in the St. Marys River; for instance, discharges from the Algoma Steel Corporation contributed polycyclic aromatic hydrocarbons (PAHs) while six outfalls into the river introduced suspended solids and coal tar compounds (ammonia, cyanide, oil, grease and phenols) (Ripley et al., 2011). Sewage plants and the paper industry in the region were also detrimental to water quality (Ripley et al., 2011). A leather tannery operated from 1900 to 1958 on the U.S. side, which contributed to the release of chromium, cyanide, sulfide, and mercury into the system (Ripley et al., 2011). Previous water quality assessments have reported elevated levels of PAHs, phenols, iron, cyanide, ammonia, zinc and sulfide downstream of Ontario sources, as well as high phosphorous levels in certain areas (St. Marys River RAP, 1992).

In this study, we used tumor incidence data of white suckers from three sites: Batchawana Bay (characterized as the reference site), Bellevue Marina (exposed site), and Partridge Point (exposed site) (Fig. 1). A fourth site, St. Joseph Island, was identified as the near-field site, but was not considered in the present analysis due to data scarcity. Batchawana Bay is located in the Batchawana Bay Provincial Park, operated by the Ontario Ministry of Natural Resources. Partridge Point is located near a sewage plant outfall, while Bellevue Marina is a public marina in Sault Ste. Marie, Ontario. A total of 239 samples from the year 2009 were used (Table 2; however, two samples were discarded from Bellevue Marina due to missing covariate information); 100 samples were obtained from Batchawana Bay and 139 from the two exposed sites. For each sample, we obtained information on the incidence of four neoplasms (hepatocellular adenoma, hepatocellular carcinoma, cholangioma and cholangiocarcinoma), five pre-neoplasms (bile duct hyperplasia, basophilic focus, eosinophilic focus, clear cell focus, and vacuolated focus) and eight lesions (not considered in this study), all of which were characterized by ones (1 s) and zeroes (0 s) to indicate presence and absence, respectively. However, many of these neoplasms and pre-neoplasms were not found in adequate numbers in both the reference and exposed sites, and thus only the forms presented in

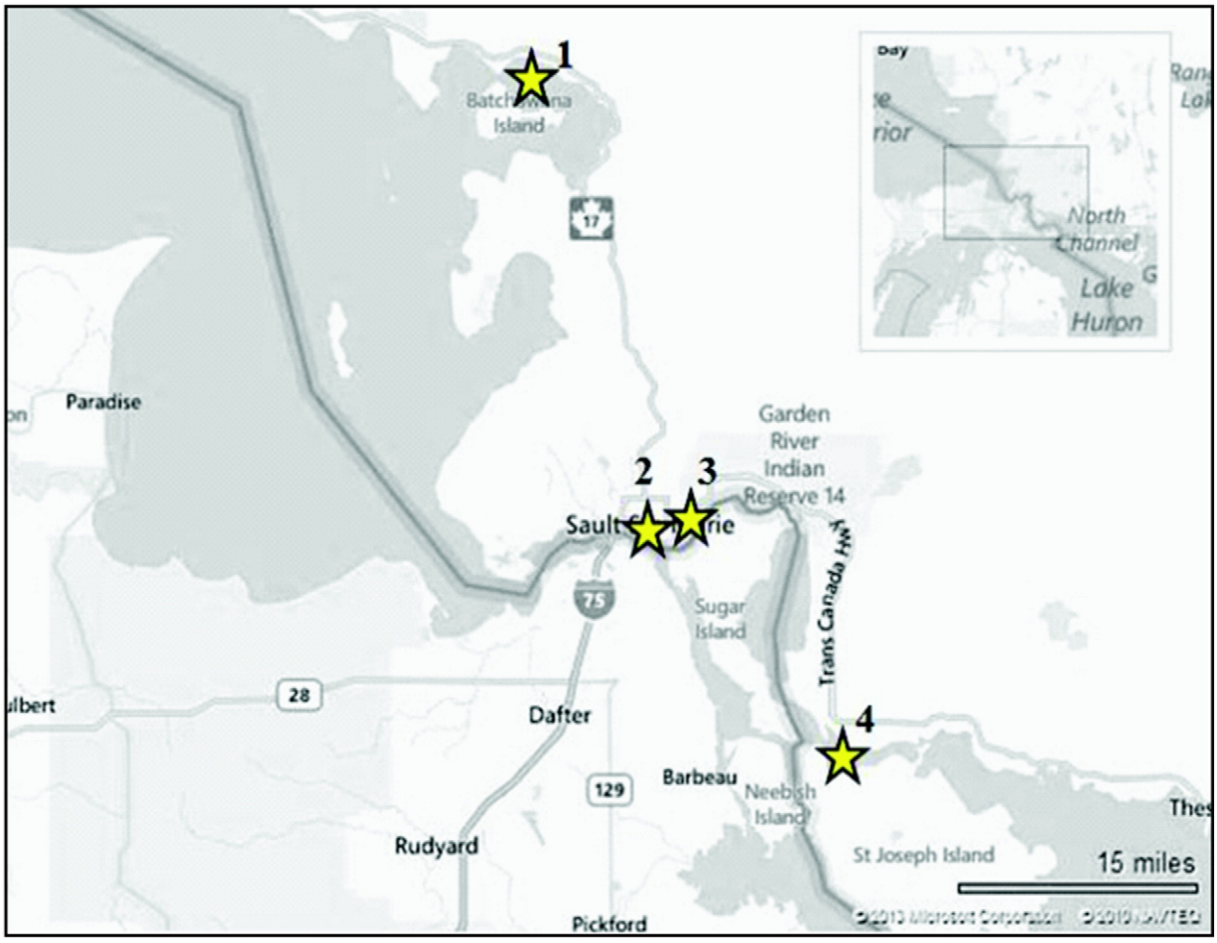

Fig. 1. Map of St. Marys River white sucker sampling sites: 1) Batchawana Bay; 2) Bellevue Marina; 3) Partrige Point; 4) St. Joseph Island.

Table 2 were examined. Definitions of each of the neoplastic tumors and pre-neoplastic forms considered are provided in Table 1, while Electronic Supplementary Material (ESM) Table S1 also gives the average age, weights and lengths of the white sucker examined.

Bayesian modeling framework

Our first model (Bernoulli model) postulates that the examination of tumor incidence in a data set resembles a Bernoulli process, meaning that the collected samples represent a sequence of independent identically distributed Bernoulli trials. Simply put, each time we collect a fish sample the outcome of that observation, tumor occurrence or not, is independent from the previous samples, while the probability p that a fish has a tumor can be determined by a series of potentially important causal factors, such as the fish age, fork length, liver weight, gonad weight, or total fish weight. The causal association between the probability that a fish has a tumor and its age and/or morphological characteristics was modeled using logistic regression (Pinkney et al., 2009; Rutter, 2010). Thus, the first model can be summarized as follows:

$$\begin{aligned} \text{Tumor}_{\text{obs}(i)} | p_i\left(\beta_0, \beta_j, x_{ij}\right) &\sim \text{Bernoulli}(p_i) \\ \text{logit}(p_i) &= \beta_0 + \sum_{j=1}^{k} \beta_j x_{ij} \\ \beta_0, \beta_j &\sim N(0,\ \ 10,000) \quad j = 1, \ldots, k \end{aligned} \tag{1}$$

Table 1
Brief descriptions of the neoplasm and pre-neoplasms forms examined in this study.

	Name	Description	Organ affected	Ref.
Neoplasms	Hepatocellular adenoma	Benign or noninvasive hepatic neoplasm	Liver	1
	Hepatocellular carcinoma	Malignant or invasive hepatic neoplasm	Liver	1
	Cholangioma	Benign bile duct neoplasm	Liver	1
	Cholangiocarcinoma	Malignant bile duct neoplasm	Liver	1
Pre-neoplasms	Bile duct hyperplasia	Non-neoplastic lesion often shown through an increased number of bile ducts compared to normal liver	Liver	2, 3
	Basophilic focus	One of the foci of cellular alteration that exhibits increased basophilic staining compared to adjacent cells	Liver	2, 3
	Eosinophilic focus	One of the foci of cellular alteration that exhibits increased eosinophilic staining compared to adjacent cells	Liver	2, 3
	Clear cell focus	One of the foci of cellular alteration	Liver	2
	Vacuolated cell focus	One of the foci of cellular alteration that exhibits hepatocytes with clear cytoplasmic vacuoles of varying sizes	Liver	2, 3

[1] Rafferty, S. D., Blazer, V.S., Pinkney, A.E., Grazio, J.L., Obert, E.C., and Boughton, L. 2009. A historical perspective on the "fish tumors or other deformities" beneficial use impairment at Great Lakes Areas of Concern. J. Great Lakes Res. 35, 496–506.
[2] Blazer, V.S., Rafferty, S.D., Baumman, P.C., Smith, S.B., and Obert, E.C. 2009b. Assessment of the "fish tumors or other deformities" beneficial use impairment in brown bullhead (*Ameiurus nebulosus*): II. Liver neoplasia. J. Great Lakes Res. 35, 527–537.
[3] Blazer, V.S., Fournie, J.W., Wolf, J.C., and Wolfe, M.J. 2006. Diagnostic criteria for proliferative hepatic lesions in brown bullhead (*Ameiurus nebulosus*). Dis. Aquat. Org. 72, 19–30.

where $\text{Tumor}_{\text{obs}(i)}$ denotes the tumor occurrence (1 or 0) in the ith fish individual; x_{ij} corresponds to the standardized value of the j covariate in the same individual; and β_0 and β_j are the regression coefficients which were assigned flat (or diffuse) normal prior distributions with mean 0 and variance 10,000 or $N(0, 10{,}000)$.

Our second statistical formulation (Zero-Inflated Poisson model) is based on a Zero-Inflated probability distribution that allows for frequent zero-valued observations. The Zero-Inflated (ZIP) Poisson model is a statistical description of a random event, containing excess zero-count data per unit of time/space or within a fixed interval of a relevant covariate. The model dissects the studied event (tumor occurrence) into two components that correspond to two zero generating processes. The first process reflects the adequacy of the sample size (i.e., sampling error) and is governed by a binary distribution that generates structural zeroes, while the second mechanism represents the tumor formation rate and is governed by a Poisson distribution that generates counts, some of which may be zero. In the present model, the probability p of the former process is associated with the sampling frequency of a fixed range of important covariates (e.g., age, fork length, weight), and the mean λ of the latter process depends on the actual values of the same causal factors. The two model components can be described as follows:

$$\begin{gathered}
\text{Tumor}_{\text{counts}(i)}|\lambda_i\left(\beta_0,\beta_j,\hat{x}_{jn}\right);p_i(u,Y_i) \sim \begin{cases}\text{Poisson}(\lambda_i) & \text{with probability } p_i\\ 0 & \text{with probability } 1-p_i\end{cases}\\
\log(\lambda_i)=\beta_0+\sum_{j=1}^{k}\beta_j\hat{x}_{jn}\\
\hat{x}_{jn}\sim U\left(\bar{x}_{jn}-\Delta x_j/2,\bar{x}_{jn}+\Delta x_j/2\right)\\
p_i=\exp(-u/Y_i)\\
u\sim U(2,5)\\
\beta_0,\beta_j\sim N(0,\ 10{,}000)\\
i=1,\ldots,I \text{ where } I=\prod_{j=1}^{k}N_j \text{ and } j=1,\ldots,k
\end{gathered}\tag{2}$$

where $\text{Tumor}_{\text{counts}(i)}$ denotes the tumor counts within the ith combination of the N_j classes of the k covariates; $\hat{x}_{jn}$ is a random uniform draw from the n class of the j covariate ($1 < n < N_j$), and thus the calculation of the mean tumor formation rate, λ_i, associated with the ith combination of covariate classes is not based solely on the midpoint values $\bar{x}_{jn}$ of the corresponding intervals Δx_j; Y_i corresponds to the number of samples within the ith combination of covariate classes; and u represents a coefficient that shapes the likelihood to observe fish tumors as a function of the number of samples collected. The latter parameter was assigned a uniform distributions with lower and upper bounds set equal to 2 and 5, or $U(2,5)$, to express our prior belief about the probability to observe a tumor with different sampling intensity levels.

The third statistical formulation (Binomial–Poisson model) similarly postulates that the sampling intensity is the primary factor that determines the accuracy of tumor observations. In this case though, we specify a binomial model in which the observed tumor counts, $\text{Tumor}_{\text{counts}(i)}$, within the ith combination of classes covariate, are conditioned upon the actual (but unobserved) tumor occurrences, $\text{Tumor}_{\text{latent}(i)}$, and the probability of detection, $p_i(u,Y_i)$:

$$\begin{gathered}
\text{Tumor}_{\text{counts}(i)}|\text{Tumor}_{\text{latent}(i)},\lambda_i\left(\beta_0,\beta_j,\hat{x}_{jn}\right),p_i(u,Y_i)\sim \text{Binomial}\left[\text{Tumor}_{\text{latent}(i)},p_i(u,Y_i)\right]\\
\text{Tumor}_{\text{latent}(i)}|\lambda_i\left(\beta_0,\beta_j,\hat{x}_{jn}\right)\sim\text{Poisson}(\lambda_i)\\
\log(\lambda_i)=\beta_0+\sum_{j=1}^{k}\beta_j\hat{x}_{jn}\\
\hat{x}_{jn}\sim U\left(\bar{x}_{jn}-\Delta x_j/2,\bar{x}_{jn}+\Delta x_j/2\right)\\
p_i=\exp(-u/Y_i)\\
u\sim U(2,5)\\
i=1,\ldots,I \text{ where } I=\prod_{j=1}^{k}N_j \text{ and } j=1,\ldots,k\\
\beta_0,\beta_j\sim N(0,\ 10{,}000)
\end{gathered}\tag{3}$$

The actual occurrence of tumors, $\text{Tumor}_{\text{latent}(i)}$, is specified as a Poisson process, conditional on the average (or expected) tumor formation rate, λ_i, related to the ith combination of covariate classes, which in turn is determined by the causal log-linear model used with the Zero-Inflated Poisson model.

The optimal combination of covariates with each of the three model categories was determined using the deviance information criterion (DIC), a Bayesian measure of model fit and complexity (Spiegelhalter et al., 2003). DIC is given by

$$\text{DIC}=\overline{D(\theta)}+p_{\text{D}} \tag{4}$$

where $\overline{D(\theta)}$ is the posterior mean of the deviance, a measure of residual variance in data conditional on the parameter vector θ. The deviance is defined as $-2\log(\text{likelihood})$ or $-2\log[p(y|\theta)]$; p_{D} is a measure of the "effective number of parameters" and corresponds to the trace of the product of Fisher's information and the posterior covariance. It is specified as the posterior mean deviance of the model $\overline{D(\theta)}$ minus the point estimate of the model deviance when using the means of the posterior parameter distributions, i.e., $p_{\text{D}}=\overline{D(\theta)}-D(\overline{\theta})$. Thus, this Bayesian model comparison first assesses model fit or model "adequacy" (sensu Spiegelhalter et al., 2003), $\overline{D(\theta)}$, and then penalizes complexity, p_{D}. A smaller DIC value indicates a "better" model.

Model computations

Using Markov-chain Monte Carlo (MCMC) simulations (Gilks et al., 1998), we obtained sequences of realizations from the model posterior distributions. We used a general normal-proposal Metropolis algorithm that is based on a symmetric normal proposal distribution, whose standard deviation is adjusted over the first 4000 iterations, so that the acceptance rate ranges between 20 and 40%. For each analysis, we used three chain runs of 50,000 iterations, keeping every 10th iteration (thin of 10) to minimize serial correlation. Samples were taken after the MCMC simulation converged to the true posterior distribution; convergence was assessed using the modified Gelman–Rubin convergence statistic (Brooks and Gelman, 1998). The convergence of the sequences occurred fairly quickly (~5000 iterations), and thus our summary statistics reported are based on the remaining draws. Finally, to ensure the accuracy of our posterior parameter values, we confirmed that the Monte Carlo error for parameters (an estimate of the difference between the true posterior mean and the mean of the sampled values) was less than 5% of the sample standard deviation (Spiegelhalter et al., 2002).

Results

Basic statistical trends

The total neoplasm and pre-neoplasm rates were higher for the exposed relative to the reference site (Table 2). For the exposed site, the total neoplasm prevalence was 10.6% (15/141) and the pre-neoplasm occurrence rate was 17.7% (25/141). In contrast, the reference site displayed a neoplasm frequency of 5% (5/100) and pre-neoplasm frequency of 12% (12/100). These relatively high neoplasm percentages suggested that the Batchawana Bay is not likely the most suitable reference site for St. Marys River. The establishment of more appropriate baseline conditions may require pooling data from several pristine sites and thus effectively balancing the elevated tumor rates occasionally experienced in a single location. For illustration purposes, we included 100 additional samples from Mountain Bay in Lake Superior (total $n = 200$ white sucker samples), which is located close to a small undeveloped nature reserve, the Gravel River Provincial Park. The pooled reference site was characterized by a 2.5% neoplastic rate (5/200), as no neoplasms were recorded in the 100 additional samples from Mountain Bay (last column of Table 2). Pre-neoplasm counts in the new reference

Table 2
Neoplasm and pre-neoplasm counts in St. Marys white sucker along with the pooled reference site that includes Mountain Bay.

	Exposed sites		Reference site		Pooled reference site	
Tumor name	Count	Total *n*	Count	Total *n*	Count	Total *n*
Hepatocellular adenoma	1	141	0	100	0	200
Hepatocellular carcinoma	3	141	4	100	4	200
Cholangioma	4	141	0	100	0	200
Cholangiocarcinoma	8	141	1	100	1	200
Total neoplasms	15	141	5	100	5	200
Bile duct hyperplasia	8	141	2	100	5	200
Basophilic focus	2	141	1	100	5	200
Eosinophilic focus	0	141	1	100	1	200
Clear cell focus	1	141	0	100	0	200
Vacuolated cell focus	17	141	9	100	14	200
Total pre-neoplasms	25	141	12	100	24	200

pool were now 24/200, which came to the exact pre-neoplasm rate identified in the original reference site (12%). Note that the calculations of total neoplasms and pre-neoplasms refer to how many fish samples were identified as having at least one neoplastic/pre-neoplastic form from each site (a binary calculation), and thus the total numbers may not align with the individual counts of tumor forms reported in Table 2. As noted earlier, we only selected neoplastic/pre-neoplastic forms that had significant numbers in each site, as there were many forms that had very low occurrence and were thus not considered. In the exposed sites, the most prevalent neoplastic form was cholangiocarcinoma ($n = 8$), followed by cholangioma ($n = 4$) and hepatocellular carcinoma ($n = 3$). The most prevalent preneoplastic form was the vacuolated cell foci, which was observed 17 times. Bile duct hyperplasia was also quite common, manifested 8 out of 141 times, or 6%. In contrast, the most prevalent neoplastic form in the reference site was the hepatocellular carcinoma ($n = 4$), with only one instance of cholangiocarcinoma (Table 2). The pre-neoplasm patterns were similar to the exposed site, with the highest number seen for vacuolated cell focus ($n = 9$), followed by bile duct hyperplasia. Across all sites, hepatocellular adenoma was found in consistently low numbers (one in exposed and zero in reference sites), with the pre-neoplastic forms eosinophilic focus and clear cell focus also being negligible in terms of their total numbers.

Having established the dominant tumor and pre-tumor forms, we then examined potential covariates for our models by investigating the relationships between five white sucker characteristics: age, fork length, total weight, gonad weight, and liver weight. The average age of white sucker was higher in the exposed sites (11.01 ± 4.11 years) compared to the reference site (9.81 ± 3.09 years), with sampled females being older than males in both sites (Table S1). Fork lengths were relatively comparable between the two sites (43.64 ± 3.77 cm in exposed; 44.30 ± 3.86 cm in reference), while total weight and gonad weight were lower in the exposed compared to the reference site (Table S1). Finally, liver weight was slightly higher in the exposed sites (mean 18.74 ± 8.04 g) relative to the reference site (17.20 ± 7.30 g). The marginal distributions of each of the variables can also be seen in the diagonals of the matrices presented in Fig. 2.

According to the Spearman rank correlation coefficient values, all relationships between the variables (original scale) were significant (ESM Table S3). The strongest relationships in both sites were between fork length and total weight (0.86 in exposed and 0.96 in reference). As expected, there were similarly strong correlations between age and fork length (0.80 in exposed and 0.83 in reference), between total weight and gonad weight (0.72 in exposed and 0.82 in reference) and between total weight and liver weight (0.85 in exposed and 0.78 in reference). Fig. 2 depicts the distribution of each variable and the bi-variate scatterplots, again reflecting the strong relationships between fork length and total weight. The relationships between age and each of the other variables appears less definite, as shown by the increased scatter in the associated plots and the presence of some outliers. The scatterplots also indicate stronger relationships between most of the variables in the reference site compared to the exposed sites, a pattern which is corroborated by the Spearman coefficient values. We also examined how do these five physical characteristics vary between fish with ("tumor fish") and without ("non-tumor fish") neoplasms/pre-neoplasms (Fig. 3). It can be clearly seen that "tumor fish" was typically characterized by higher ages and greater fork lengths, regardless of the tumor form examined. The relationships with weights were less straightforward, as there was a case where the "tumor fish" had lower gonad weight (i.e., cholangioma in exposed sites) and a few instances where the median weights were almost identical between the two states.

Fish tumor modeling

The most parsimonious fish tumor models are presented in Table 3, although none of the combination of covariates examined received DIC values (>2 difference relative to the selected model) that suggest considerably less support (Spiegelhalter et al., 2002). We ended up with six models for each statistical configuration, with cholangioma, cholangiocarcinoma, bile duct hyperplasia and total neoplasms examined in the exposed sites, and bile duct hyperplasia and total pre-neoplasms examined in the reference site. The absence of models for the total neoplasms in the exposed site and the total pre-neoplasms in the reference site was due to the low degree of identification of the slope parameters ($\beta_{SD}/\beta_{mean} > 1$) associated with any of the covariates considered. The latter pattern may stem from the fact that the predictor variables used are intrinsically collinear, as they represent different manifestations of the same underlying process (i.e., fish aging). Thus, there were instances when the posterior coefficients were characterized by inflated standard errors, which may have been an impediment for identifying the relative role of important factors, even if they were truly influential. In the models qualified, age was always an important covariate, while the second one was fork length, gonad weight or liver weight, depending on the tumor form examined. In the exposed site, age and gonad weight was the covariate combination used for cholangioma while total neoplasms were consistently based on age and fork length. In the reference site, age and liver weight was the covariate combination with the strongest signature on the bile duct hyperplasia and total pre-neoplasms. The parameter posteriors for each of the models developed are presented in ESM Table S2.

We first examined the frequency histograms of the predicted tumor probability values for the different covariate combinations considered with our Bernoulli model (Fig. 4). To exploit more effectively the benefits of our modeling exercise for policy decisions, we include a dashed line in Fig. 4 that signifies a probability value of 10%, as the maximum acceptable tumor incidence risk for each specimen examined. In the exposed sites, 94% of the mean predicted occurrence rates for cholangioma were below the 10% benchmark, thus indicating low overall likelihood of encountering this tumor form (Fig. 4a). In contrast, cholangiocarcinoma was characterized by lower number of cases below the cut-off point, as 81% of the values were below the 10% line and the thicker right tail of the distribution was indicative of higher risks for this neoplasm form (Fig. 4b). Likewise, bile duct hyperplasia had more instances of exceedance than cholangioma, with 87% of the values below 10% (Fig. 4c). The distribution of tumor probabilities for total neoplasms was characterized by a thicker right tail, with only 65% of the values falling under the 10% line (Fig. 4d). In the reference site, the patterns for bile duct hyperplasia were characterized by >90% of the mean predicted incidence rates falling below the 10% cut-off level (Fig. 4e). In contrast, the predicted patterns for total pre-neoplasm indicated that about half of the cases examined fell under the 10% benchmark, and thus the distribution of the mean predictions suggests relatively high probabilities for total pre-neoplasms in the reference site (Fig. 4f). In a similar manner, the encircled numbers

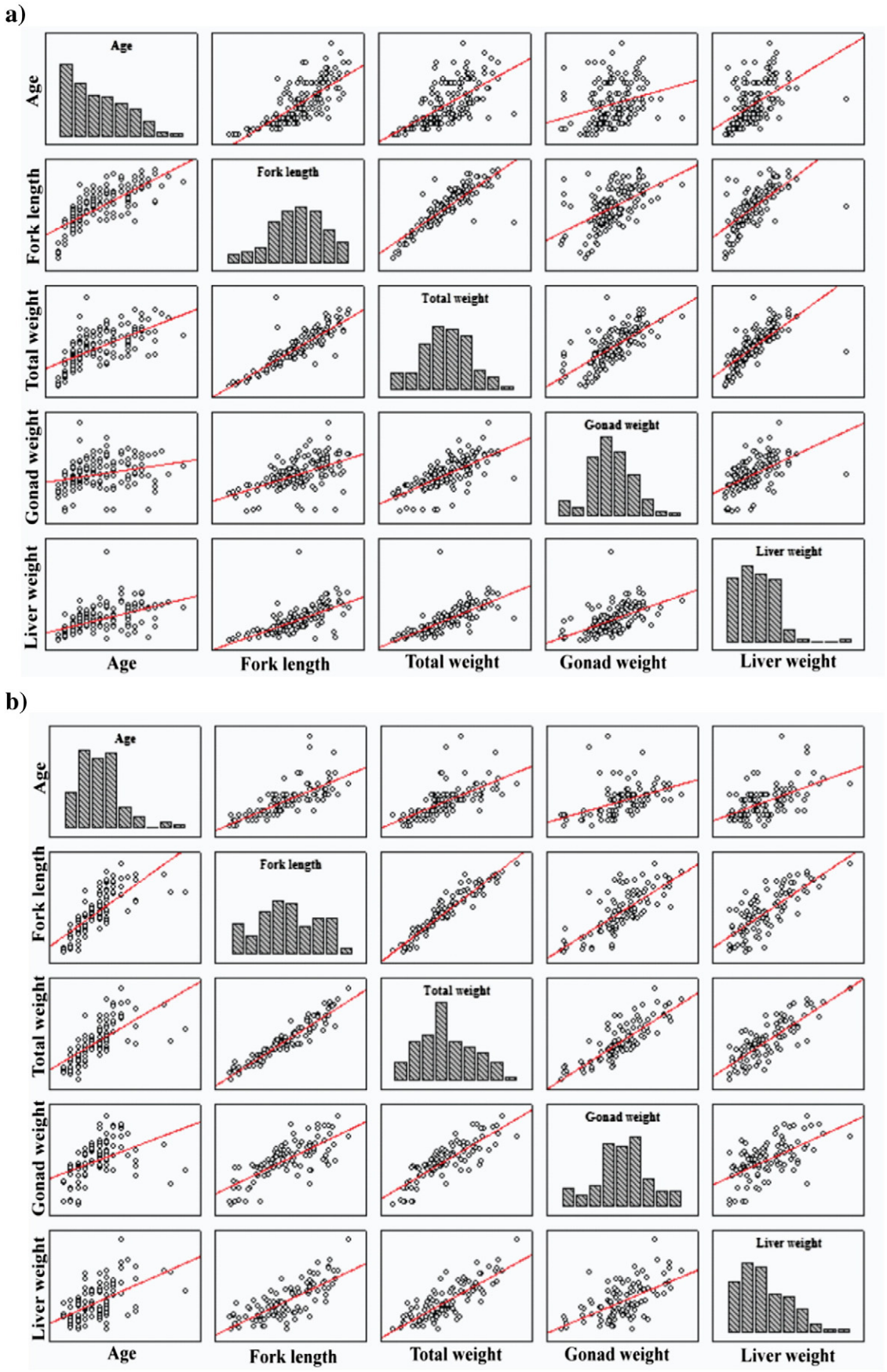

Fig. 2. Correlation matrices for white sucker physical characteristics across a) exposed sites and b) reference site in St. Marys River. Bar graphs give frequency histograms for fish characteristics at each site.

represent the probability levels associated with a more stringent criterion that stipulates <5% likelihood of tumor exceedance in each fish sampled.

With both the Zero-Inflated Poisson and the Binomial–Poisson statistical formulations, we specified intervals (or bins) for each of the covariates considered (age, fork length, gonad weight, or liver weight), and we present the scatterplots depicting the predicted "true" tumor occurrences, $Tumor_{latent}$, against the increasing age (4–24 years), gonad weight (0–160 g), fork length (32–52 cm), and liver weight (0–45 g) for the latter model. In the exposed site, the predicted occurrences of cholangiomas remained quite low up to age-20, with an abrupt rise in predictions for older fish (Fig. 5a, left panel). Notably, the presence of one unusually high prediction for age-18 fish is associated with a similar outlier in the gonad weight panel, which incidentally yielded a high prediction of ~40 tumors (Fig. 5a, right panel). The pattern of predicted tumors as we increased the gonad weight was less clear, with no overt trend displayed between the two variables. In contrast, clearly identifiable patterns were seen for cholangiocarcinoma, bile duct hyperplasia and total neoplasms in the exposed sites (Figs. 5b–d, left panels). As the age of the white sucker increased, the predicted tumor occurrences sharply curved upwards after age-16 fish. Fork length, the second covariate for each of these forms, also demonstrated increasing tumor incidence rates with longer fish, while negligible tumors were predicted for fish under 36 cm (Figs. 5b–d, right panels). Interestingly, the reference site, showed greater scatter in the bile duct hyperplasia patterns (Fig. 5e, both panels). In a similar manner, tumor occurrences increased in fish after age-16, but the relationship is nowhere as clear as it was earlier. Similarly, the relationship with liver weight does indicate higher tumor counts for fish with heavier livers, but the pattern is again more scattered. Finally, the total pre-neoplasm model for the reference site again indicates a strong linkage between age and actual tumor occurrence (Fig. 5f, left panel), with total pre-neoplasm counts reaching up to 24 for age-22 fish. The results for liver weight predicted more of a steady increase in total pre-neoplasm occurrence as the weight of the white sucker livers was increased, with a few instances of high tumor rates in livers weighting between 20 and 30 g (Fig. 5f, right panel).

Discussion

Development of delisting criteria for the "fish tumors and other deformities" BUI

The development of rigorous delisting criteria for BUIs has been the subject of much discussion in recent years, given that the IJC leaves much of the responsibility to individual RAP teams (IJC, 2012). Even when guidelines are provided to instruct the individual teams, the inadequacy of such recommendations has often led to fundamentally different strategies and dissimilar delisting goals for the same BUI in various Areas of Concern (NSE, 2003). Although a certain degree of subjectivity is inherent in any scientific venture, the suitability of selected reference (or "unimpaired") sites has been one of the controversial issues as the guidelines on what constitutes an unimpaired site are decidedly unclear (Blazer et al., 2009a,b). An additional challenge when designing environmental policy is related to the growing awareness of the uncertainty in natural systems with a recent tendency towards probabilistic strategies that allow for a certain degree of violations of the targeted environmental goals (Gudimov et al., 2011). It is within this context that our Bayesian methodological framework aims to assist with the development of delisting criteria for the "fish tumors and other deformities" BUI. We present a series of models that provide probabilistic estimates of tumor incidence rates in fish populations as a function of their physical covariates, while explicitly accounting for the natural uncertainty as well as the likelihood that the available data may obfuscate our ability to impartially discern the differences between impaired and reference sites.

The "fish tumors and other deformities" BUI has been extensively debated in regards to the progress made about the histopathological, sampling, and statistical procedures (Rafferty, 2003a,b). The IJC suggests that this BUI is impaired when the incidence rate of fish tumors (or other deformities) exceeds rates at control sites or when survey data confirm the presence of neoplastic or pre-neoplastic liver tumors in bullhead or suckers. However, aside from the lack of delineation of the "unimpacted" conditions, considerable confusion exists on what should be deemed as unacceptable tumor incidence rates (Blazer et al., 2009a,b). Attempts have been made to propose direct quantitative criteria for this specific impairment, such as the proposition for the Canadian side of the St. Marys River AOC to consider as delisting goal a lower than 5% prevalence rate of total liver neoplasms in fish data sets (e.g., white suckers) with adequate sample size ($n \geq 100$) (FPS, 2010). Similarly, Baumann et al. (1996) suggested that intestinal or liver tumor prevalence greater than 5% in benthic dwelling fish constitutes impairment. Other delisting targets proposed by RAP teams are based on recording the absence of neoplastic/pre-neoplastic tumors in certain fish species, eliminating contaminants from industrial/ municipal discharges, and establishing contaminant concentrations in fish/wildlife below critical levels (IJC, 2012). Hitherto, no AOC has been successfully delisted for the fish tumors BUI, and only a handful have undertaken a comprehensive investigation of the ongoing status (Rafferty et al., 2009). There are fourteen AOCs where the fish tumors and other deformities BUI is impaired, with Presque Isle Bay AOC and Black River (Ohio) recently listed as being "in recovery" (Rafferty et al., 2009). This designation means that all active remediation is complete and the focus now is on monitoring to what extent the sites respond to the actions taken (Rafferty et al., 2009).

Fish tumor patterns in St. Marys River

Quite recently, a series of papers have examined long-term changes in the fish community as well as fisheries assessment plans in the St. Marys River Area of Concern (Fielder et al., 2007; Pratt and O'Connor, 2011; Schaeffer et al., 2011). The fish tumors and other deformities BUI was initially listed as impaired in the St. Marys River AOC due to incidences of hepatic cancer in white suckers and brown bullheads (FPS, 2010). The river's white suckers were also previously sampled in 1988, with results revealing a lip/body papilloma prevalence of 9.1% (Smith, unpublished data). In the context of our study, our results reveal liver neoplasm rates of 10.6% for white sucker from the pooled exposed site, which is well over any of the impairment benchmarks proposed in the literature. Clearly, the issue of fish tumors is still of concern within the St. Marys River, and further action or time may be necessary to designate this BUI as not impaired.

Our initial exploratory analysis of neoplasm/pre-neoplasm prevalence yielded a few key observations regarding the nature of our data set. First, we treated the two exposed sites as one "exposed" pool, although the site that contributed a greater percent of neoplasms was Bellevue Marina (12 neoplasms) as compared to Partridge Point, near a municipal sewage plant (only 3 neoplasms). This is somewhat surprising, as the sewage plant outfall was expected to contribute a greater share of tumor-fish. PAHs are the carcinogens of concern in the St. Marys system, occurring in higher levels in the Bellevue sediments (near the Algoma Steel coking facility) than in the sediments near Partridge Point. Thus, one would expect the Bellevue sucker population to have more tumors than the sucker population at Partridge Point (assuming minimal mixing). In addition, the age distributions (not presented here) indicated that Partridge Point is characterized by a more

Fig. 3. Box-plots of neoplasms and pre-neoplasms against white sucker physical characteristics (age, liver weight, gonad weight, and fork length), for both exposed and reference sites in St. Marys River. Combinations shown are those presented in the models. A zero (0) on the *x*-axis of the plots indicates no occurrence while a one (1) indicates occurrence.

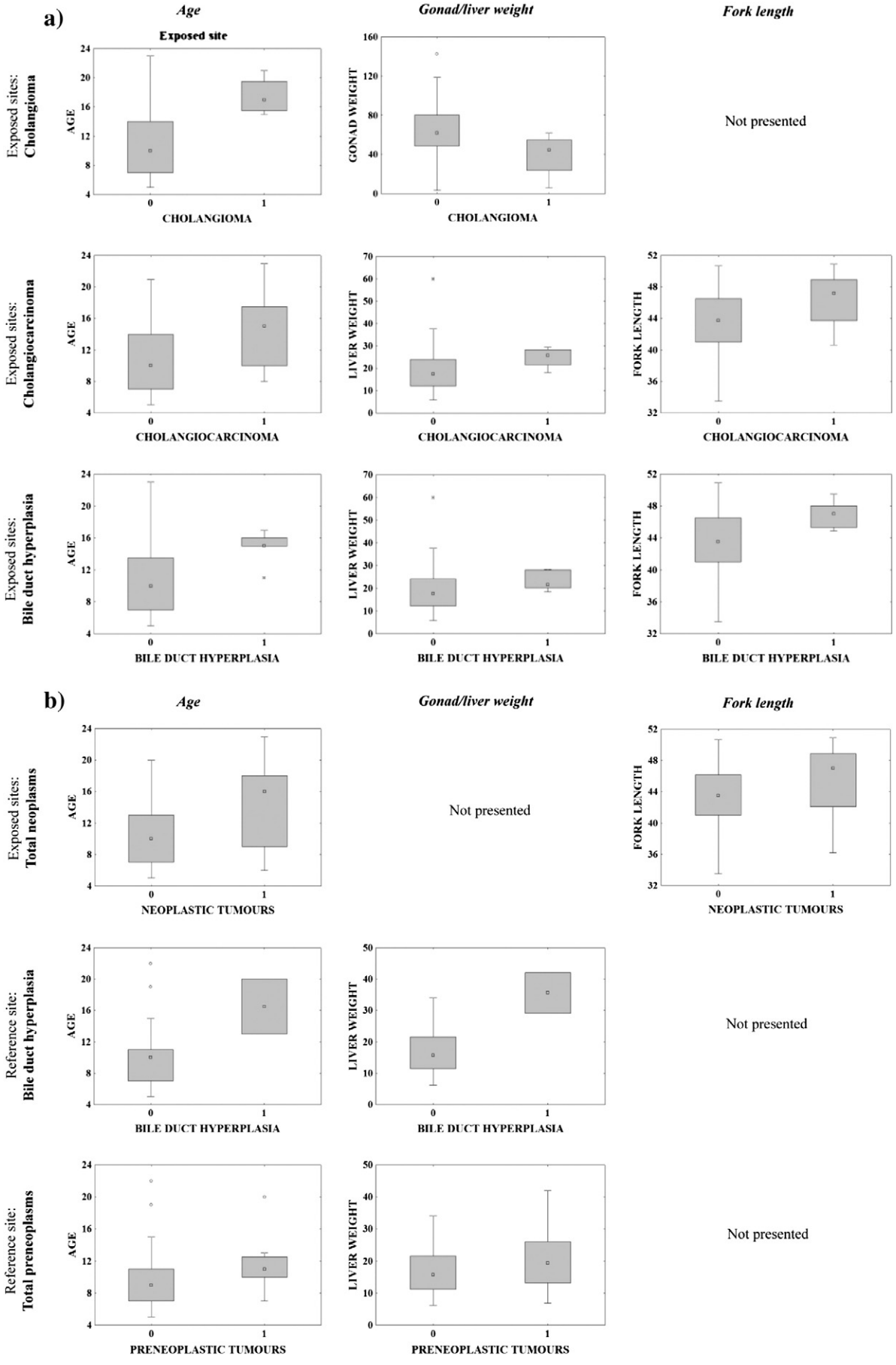
a)
Age
Gonad/liver weight
Fork length
Exposed site
Exposed sites: Cholangioma
AGE
GONAD WEIGHT
CHOLANGIOMA
Not presented
Exposed sites: Cholangiocarcinoma
LIVER WEIGHT
FORK LENGTH
CHOLANGIOCARCINOMA
Exposed sites: Bile duct hyperplasia
BILE DUCT HYPERPLASIA
b)
Exposed sites: Total neoplasms
NEOPLASTIC TUMOURS
Reference site: Bile duct hyperplasia
Reference site: Total preneoplasms
PRENEOPLASTIC TUMOURS

Table 3
The most parsimonious models for different neoplasms and pre-neoplasms, based on the use of the deviance information criterion.

	Exposed site	Reference site
Model one		
Cholangioma	Age + gonad weight	N/A
Cholangiocarcinoma	Age + liver weight	N/A
Bile duct hyperplasia	Age + fork length	Age + liver weight
Total neoplasms	Age + fork length	N/A
Total pre-neoplasms	N/A	Age + liver weight
Model two		
Cholangioma	Age + gonad weight	N/A
Cholangiocarcinoma	Age + liver weight	N/A
Bile duct hyperplasia	Age + liver weight	Age + liver weight
Total neoplasms	Age + fork length	N/A
Total pre-neoplasms	N/A	Age + liver weight
Model three		
Cholangioma	Age + gonad weight	N/A
Cholangiocarcinoma	Age + fork length	N/A
Bile duct hyperplasia	Age + fork length	Age + liver weight
Total neoplasms	Age + fork length	N/A
Total pre-neoplasms	N/A	Age + liver weight

uniform age distribution (and thus a greater proportion of older tumor-prone fish), as compared to the Bellevue Marina's right-skewed pattern. This disparity may likely stem from the sample sizes collected, as the number of samples collected for Partridge Point was less than half of those for Bellevue Marina (Table S1). Given the recommendations for a minimum of 100 specimens (FPS, 2010), a sample size of 41 (Partridge Point) was likely not robust enough; and thus the two exposed sites were pooled together. The issue of sample sizes when monitoring for this BUI has also been raised by Blazer et al. (2009a) and later by Rutter (2010), where the authors describe the sensitivity of calculated neoplasm prevalence rates to both sample size and number of liver sections examined from the fish sampled (see also following discussion). Another key finding was that the neoplasm rate for the reference site, Batchawana Bay, was actually quite high with a total liver neoplastic rate of 5%. According to the two delisting guidelines cited earlier, this reference site could be classified as impaired. The pooled reference site was thus included in aspects of our analyses, whereby the inclusion of additional samples ($n = 100$) inflated the total count and dropped the neoplastic rate to 2.5%. The nature of assessing impairment requires setting a benchmark to compare against, and our results reiterate the importance of selecting reliable reference sites. Nonetheless, we note that the use of the "seemingly-impaired" reference site still indicates an increased frequency of tumor incidence in the exposed sites, reinforcing our earlier assertion about the fish tumor problem in white sucker.

A novel feature of our study was the inclusion of pre-neoplasms in our models, which are not usually considered. Even though pre-neoplastic lesions are not as clearly defined as neoplasms in the literature, both the foci of cellular alteration and bile duct proliferation considered here have been related to contaminant exposure in many fish species (Blazer et al., 2009b). The pre-neoplastic rates calculated were quite high (>10%) in both exposed and reference sites. Pre-neoplasms are not formally addressed in delisting criteria, but the fact that they may lead to neoplastic forms makes their monitoring important (Rafferty, 2003a) and also stresses the need to unequivocally determine which lesions are in fact pre-neoplastic in other indicator species, such as brown bullheads (Blazer et al., 2009b).

From a management perspective, the importance of allowing for some degree of violation in impaired states and the usefulness of a probabilistic framework is exemplified through our "probability distributions of the exceedance probabilities" visualizations from the first Bernoulli model (Fig. 4). Stipulating a benchmark of a 10% probability for the neoplasm/pre-neoplasm risk in each sample collected, this approach is conceptually on par with the EPA-endorsed "confidence of compliance" (Zhang and Arhonditsis, 2008). In doing so, our analysis explicitly accommodates all the sources of error (structural/parametric and data uncertainty) typically involved in any modeling exercise by shifting the focus from the mean model predictions to the fraction of predicted incidence rates that exceed a pre-specified critical risk level; namely, instead of entirely basing the inference on the predicted tumor risk for given fish characteristics, we introduce an extra dimension of uncertainty and target the probability of exceedance of an acceptable tumor risk level across all the fish sampled. In the exposed sites, the higher risks were generally evident for total neoplasms, with a larger mass falling at probabilities higher than 10%. Our model projections also reveal that trends in certain forms of liver neoplasia are more worrisome than others, such as the cholangiocarcinomas as compared to cholangiomas which in turn frequently translate to the malignant bile duct form. Hepatocellular adenomas and carcinomas, the equivalent hepatic cell forms, were not considered due to the data scarcity associated with these sites. Importantly, the assessment of the degree of impairment in an exposed site with this approach can conceivably depend on the model predictions on that site alone and thus may be disconnected from the challenging delineation of the baseline conditions. We simply have to determine a universally acceptable tumor incidence risk (5% or 10%) along with an allowable proportion of cases that can be characterized by higher risk levels, regardless of the physical characteristics of the fish sampled.

Another key finding has to do with the influence of age and other covariates on the tumor rates. Notwithstanding the possible identification issues arising from the use of collinear predictors, many of the neoplastic/pre-neoplastic forms (e.g., cholangioma, cholangiocarcinoma, bile duct hyperplasia and total neoplasms in the exposed site, total pre-neoplasms in the reference site) depicted abrupt rises in tumor predictions after either age-16 or -18 fish. The importance of age in our modeling analysis ties in well with the established literature, as there is substantial evidence that liver tumor prevalence increases with the age of fish (e.g., Baumann, 1992; Pinkney et al., 2004), although the same pattern has not consistently been seen for orocutaneous tumors (Blazer et al., 2009a; Rafferty et al., 2009). Not only are fish exposed to more contaminants year after year, there is also a latent period between induction and tumor development. Generally, neoplasia prevalence in brown bullheads increases in sexually mature fish that are older than three years and live in polluted regions; thus, field sampling procedures usually require fish of a certain length to be captured in tumor prevalence surveys to ensure the accurate detection of the prevailing trends (Rafferty and Grazio, 2006; Rafferty et al., 2009). Interestingly, the fact that the influence of the fish weight and length was weaker is not surprising, given that many studies have pointed to a stronger association with age than with other factors. Fish length can only be used as a surrogate for age in younger fish and the relationship often weakens in older fish (Rafferty, 2003b). In any event, the role of the various covariates played a key role in shaping the nature of our modeling exercise, which also recognized that the strength of the causal relationships may vary between exposed and reference sites.

Alternative Bayesian methodological frameworks

In the context of Bayesian inference, Rutter (2010) recently presented a hierarchical logistic model to assess the likelihood of tumor incidence on brown bullheads in an AOC (Presque Isle Bay, Lake Erie) in comparison with several candidate control sites. While the explicit consideration of the role of important covariates (e.g., age, gender, length, weight) is a common denominator with the present study, Rutter's (2010) hierarchical approach drew inference about the frequency of fish tumors using the same combination of predictor variables for both impaired and non-impaired sites rather than basing the spatial comparisons on the most parsimonious (and better identified) models for each site. Relative to our modeling analysis though, the scope of the hierarchical framework was broader in that the intent was to accommodate

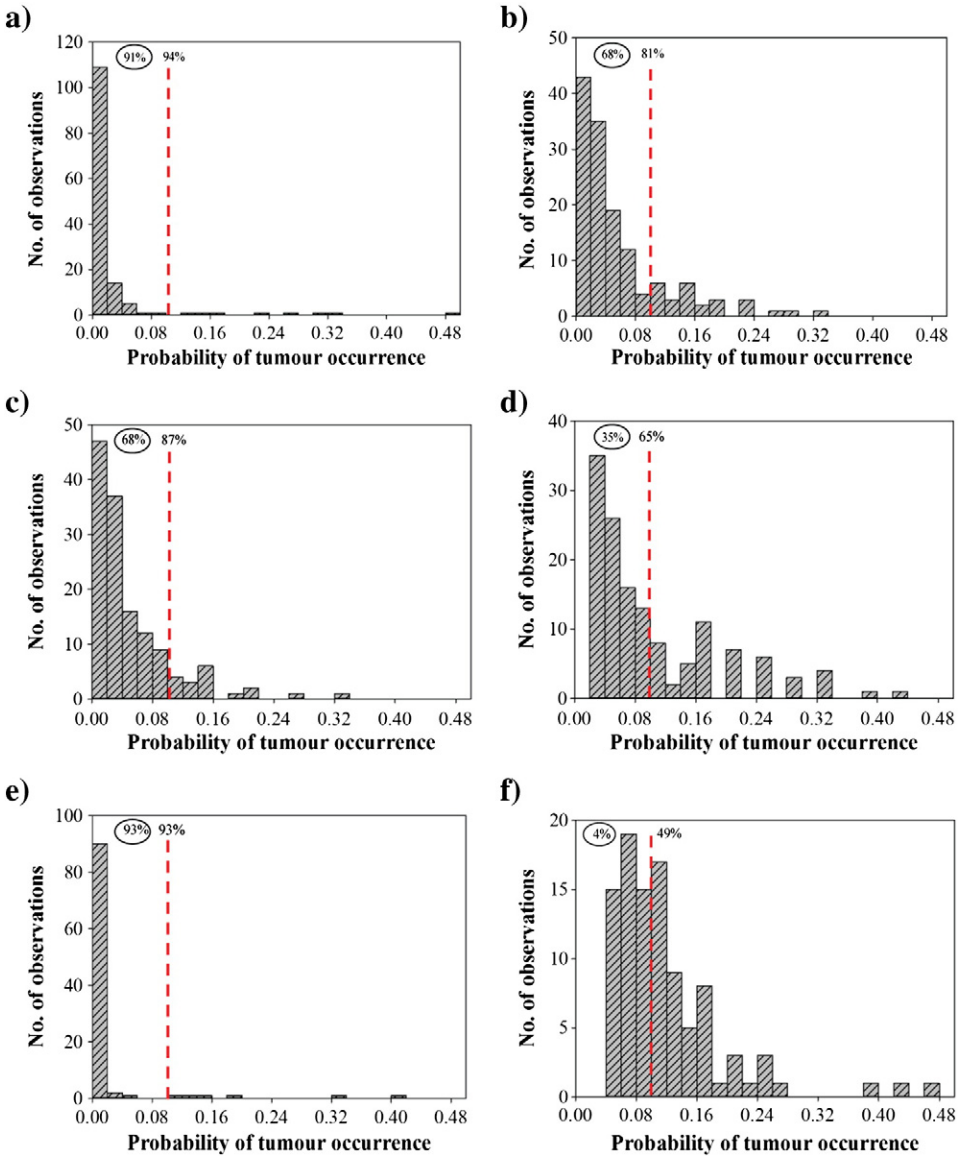

Fig. 4. Representation of tumor exceedance probabilities in St. Marys River sites, based on the Bernoulli model results. Histograms depict the likelihood of experiencing probabilities of tumor occurrence between 0 and 50%. The dotted lines represent a tentative benchmark aim of 10% probability of tumor exceedance for St. Marys white sucker, with percentage of probabilities below this line indicated to the left of each line. In a similar manner, the encircled numbers represent the probability levels associated with a more stringent criterion that stipulates <5% likelihood of tumor exceedance in each specimen examined. Panels correspond to: a) cholangioma in exposed sites; b) cholangiocarcinoma in exposed sites; c) bile duct hyperplasia in exposed sites; d) total neoplasms in exposed sites; e) bile duct hyperplasia in the reference site; and f) total pre-neoplasms in the reference site.

sampling designs in which sites are sampled over multiple years and/or at multiple sublocations within each site (Rutter, 2010). Namely, the tumor incidence rates in both exposed and reference sites were described by a hierarchical tree, characterizing the effects of a covariate at each sublocation and year in which the fish samples were collected, while a hyperparameter was specified at the top of the hierarchy to depict the lake-wide signature of the covariate. One important lesson learned was that the hierarchical model provides more realistic (larger) uncertainty estimates relative to non-hierarchical approaches that typically downplay site-level and/or year-to-year variability. Another interesting feature of Rutter's (2010) work was the standardization of the values of the covariates along with the application of Cauchy non-informative priors (Gelman et al., 2008) which in turn led to the derivation of risk assessment estimates in cases where the existing data do not contain any observed tumors. Further, the hierarchical modeling framework represents an optimal compromise between "completely pooled" (or cross-sectional) models that ignore the site-specific effects and approaches like ours that estimate separate models for each site with no data pooling (Cheng et al., 2010; Gudimov et al., 2012). By employing "partial pooling" of the available information, the hierarchical framework allows sensible comparisons among multiple sites, without the need to adjust the predictive intervals in locations with small sample sizes, e.g., the Bonferroni correction in frequentist statistics (Gelman et al., 2009).

To examine the robustness of the results presented herein, we implemented a similar hierarchical configuration of the Bernoulli model, under which the exposed and reference sites were linked through hyperparameters for the slopes, while assigning site-specific intercepts to distinguish the differences in fish tumor frequency between the two locations (see Figs. 3 & 4 in Rutter, 2010). We used the same covariates as with the original models for the total neoplasm and pre-neoplasm occurrence rates at the exposed and reference sites, respectively (Table 3). The hierarchical approach first reiterated our earlier finding that none of the existing covariates has a distinctly identifiable causal connection with the frequency of a particular tumor form at both locations (ESM Table S4). We then compared the likelihood of an "average" white

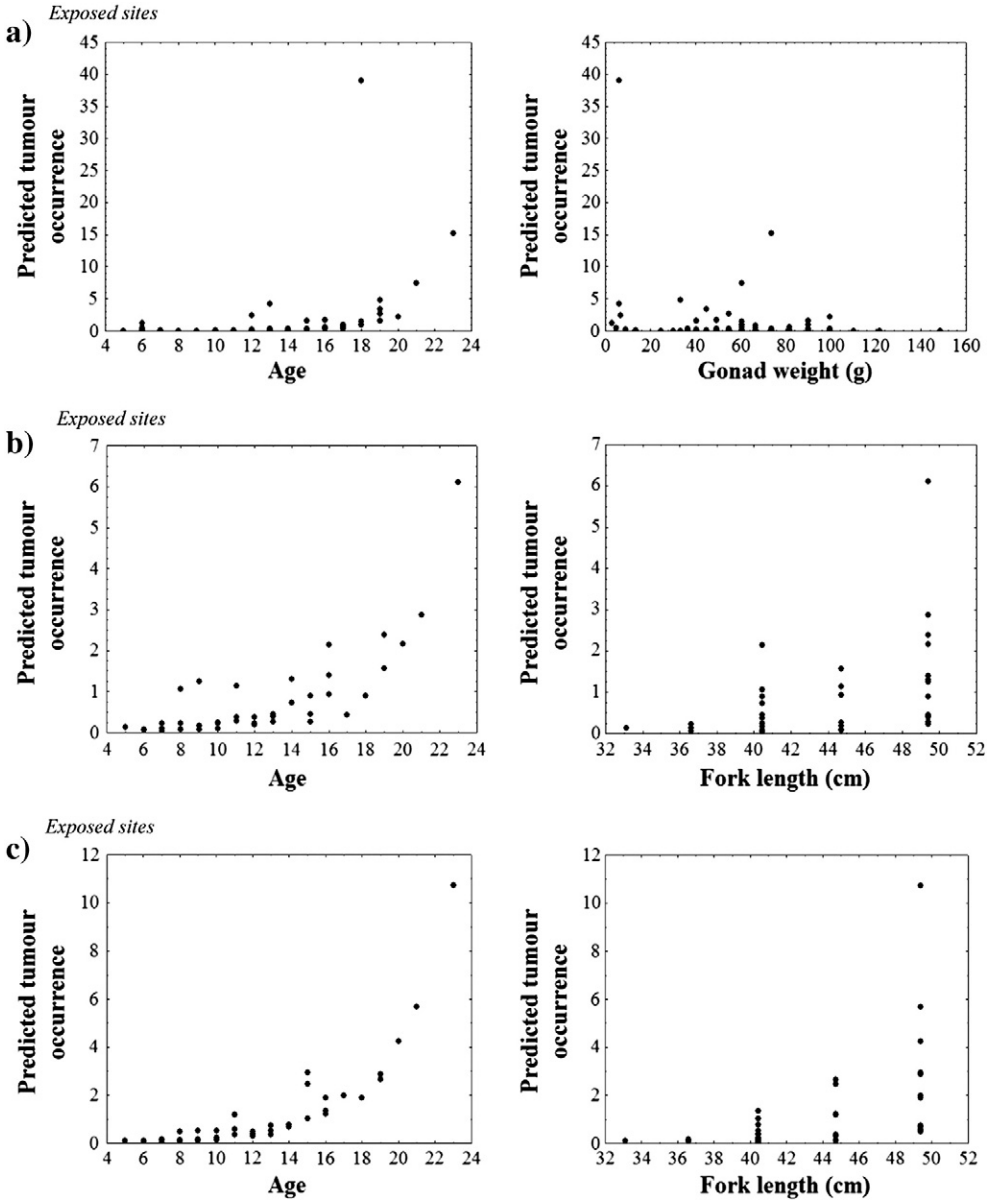

Fig. 5. Scatterplots depicting the results from the Bernoulli–Poisson model. *Y* axes represent "true" tumor occurrence in the system ($Tumor_{latent}$), against various classes of fish covariates (age, fork length, liver weight and gonad weight), plotted on the *X* axes. Panels correspond to: a) cholangioma in exposed sites; b) cholangiocarcinoma in exposed sites; c) bile duct hyperplasia in exposed sites; d) total neoplasms in exposed sites; e) bile duct hyperplasia in the reference site; and f) total pre-neoplasms in the reference site.

sucker in the exposed site having a tumor relative to the corresponding probability in the reference site over all the realizations of the parameter posterior space (Rutter, 2010). For total neoplasm data, we found that an age 10 white sucker with a fork length of 43 cm is characterized by a (−2.64%, 8.59%) frequency interval to manifest neoplasms in the exposed relative to the reference site. In a similar manner, the corresponding frequency interval for pre-neoplasms was (−3.43%, 12.22%) when considering an age 10 white sucker with a liver weight of 18.13 g. While the mainly positive differences between the two sites suggest higher incidence rates at the exposed area, a minimum tolerance level is required to infer whether these values reflect systematic trends or not (Berger and Hsu, 1996; Lauzon and Caffo, 2009). Following the procedure described by the Rutter (2010) study (see also footnote of Table S4), we specified a 12% tolerance level that reflects the belief that if two sites differ in regards to the true tumor incidence by more than 5%, then evidence of non-equivalence can only be inferred when the variability in the differences of their tumor incidence rates lies outside the ±12% uncertainty bounds. Thus, the derived differences in both neoplasm and pre-neoplasm incidence rates suggest that the exposed site is practically equivalent to the reference location.

To further discern the degree of impairment of the exposed site, we pooled the data from the two locations and used bootstrap sampling to conduct posterior simulations with the hierarchical model. In doing so, we compared the tumor incidence rates between the two sites, while eliminating the potential bias that may have been introduced by the differences in the demographics of the corresponding samples. When examined at each age (i.e., averaging the predictions over all the fork lengths measured within each age class), both the median and the 95% credible intervals suggest that the neoplasm rates are consistently higher at the exposed site compared to the reference conditions (Fig. 6a). By contrast, the predicted pre-neoplasm rates were almost similar between the two sites although the risk appears to be elevated in the reference site once white suckers of age 15 or greater are being considered (Fig. 6b). While these projections primarily reflect the

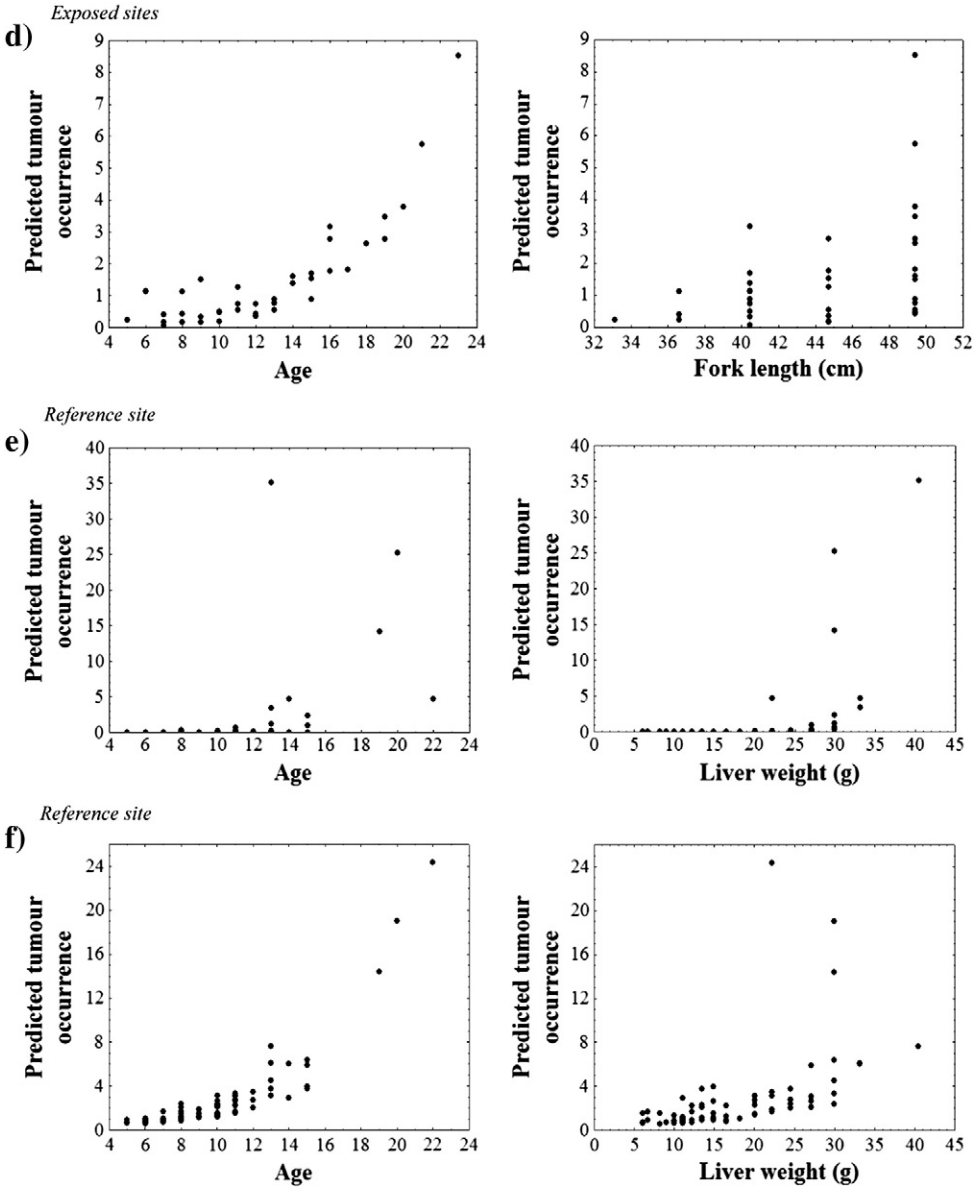

Fig. 5 (*continued*).

spatial nature of the different causal relationships as manifested in our data set, we note that the use of the criterion that stipulates the likelihood of tumor incidence to be lower than 10% for a certain fraction (or greater) of the fish samples collected appears to paint a somewhat different picture. Namely, when using the pooled sample, the mean probability of neoplasm incidence was predicted to be lower than 10% in nearly 70% and 95% of the cases in the exposed and reference sites, respectively. On the other hand, the predicted mean pre-neoplasm frequency never falls below 10% at the exposed site, whereas ≈40% of the cases are predicted to fall below the proposed cut-off level in the reference location.

In conclusion, we presented a Bayesian methodological framework that can be used to predict fish tumor incidence rates, while accommodating the emerging evidence about the causal linkages with the physical characteristics of fish (age, fork length, liver and gonad weight) and the increasing awareness on the importance of environmental policy practices that explicitly accommodate the role of uncertainty. In white sucker from the St. Marys River AOC, tumor incidence rates are generally elevated at the pooled samples from exposed sites (Bellevue Marina and Partridge Point) relative to the reference conditions (Batchawana Bay). The Bayesian counterpart of the two one-side tests for equivalence though suggests that the exposed sites are practically equivalent to the reference location in regards to the neoplasm and pre-neoplasm incidence rates. A new criterion that stipulates the likelihood of tumor incidence to be lower than 10% for a certain fraction (or greater) of the fish samples collected may be a more effective way to characterize the prevailing conditions in impacted locations. In the exposed sites, the mean probability of neoplasm incidence was predicted to be lower than 10% in 70% of the cases examined, but the predicted mean pre-neoplasm frequency never falls below the 10% cut-off level collected. The corresponding values were significantly more favorable in the reference site. We believe that the presented framework offers a rational way to evaluate fish tumor incidence rates and could play an instrumental role in guiding the formation of delisting criteria across all the impacted Great Lakes Areas of Concern.

Acknowledgments

This project has received funding support from the Ontario Ministry of the Environment. Such support does not indicate endorsement by the

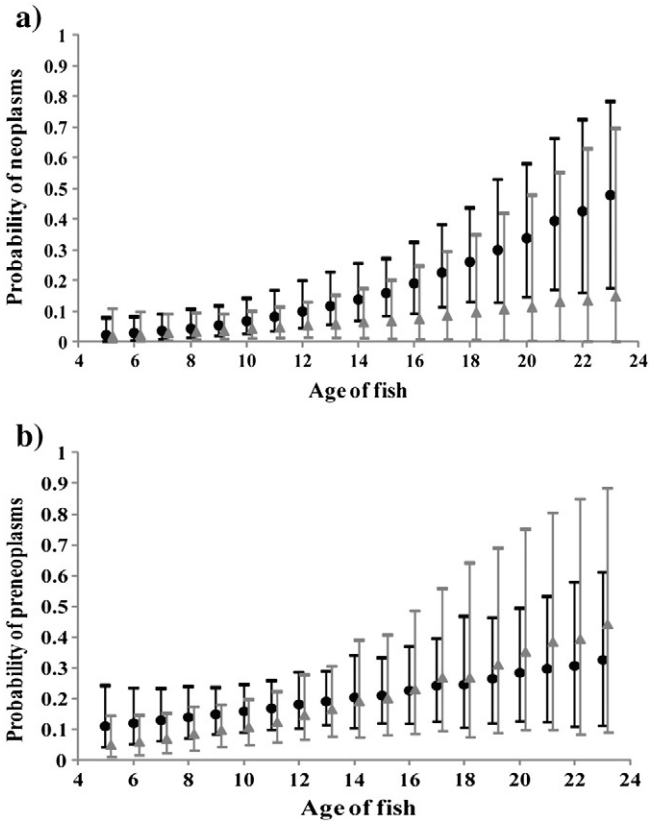

Fig. 6. Probability of (a) neoplasm and (b) pre-neoplasm incidence by age on white suckers in the exposed (black circles) and reference (gray triangles) sites in St. Marys River AOC. Estimates are based on the median and the 95% credible intervals of the posterior distribution. Posterior distributions of the predicted tumor incidence at each age are based on the mean observed fork length (neoplasm) and liver weight (pre-neoplasm) at each age and the hierarchical configuration of our Bernoulli model.

ministry of the contents of the study. All the material pertinent to this analysis is available upon request from the corresponding author.

Appendix A. Supplementary data

Supplementary data to this article can be found online at http://dx.doi.org/10.1016/j.jglr.2014.04.003.

References

Baumann, P.C., 1992. The use of tumors in wild populations of fish to assess ecosystem health. J. Aquat. Ecosyst. Health 1, 135–146.

Baumann, P.C., Harshbarger, J.C., 1995. Decline in liver neoplasms in wild brown bullhead catfish after coking plant closes and environmental PAHs plummet. Environ. Health Perspect. 103 (2), 168–170.

Baumann, P.C., Harshbarger, J.C., 1998. Long term trends in liver neoplasm epizootics of brown bullhead in the Black River, Ohio. Environ. Monit. Assess. 53, 213–223.

Baumann, P.C., Smith, I.R., Metcalfe, C.D., 1996. Linkages between chemical contaminants and tumors in benthic Great Lakes fish. J. Great Lakes Res. 22 (2), 131–152.

Berger, R.L., Hsu, J.C., 1996. Bioequivalence trials, intersection-union tests, and equivalence confidence sets. Stat. Sci. 11, 283–319.

Blazer, V.S., Rafferty, S.D., Baumman, P.C., Smith, S.B., Obert, E.C., 2009a. Assessment of the "fish tumors or other deformities" beneficial use impairment in brown bullhead (*Ameiurus nebulosus*): I. Orocutaneous tumors. J. Great Lakes Res. 35, 517–526.

Blazer, V.S., Rafferty, S.D., Baumman, P.C., Smith, S.B., Obert, E.C., 2009b. Assessment of the "fish tumors or other deformities" beneficial use impairment in brown bullhead (*Ameiurus nebulosus*): II. Liver neoplasia. J. Great Lakes Res. 35, 527–537.

Borsuk, M.E., Stow, C.A., Reckhow, K.H., 2002. Predicting the frequency of water quality standard violations: a probabilistic approach for TMDL development. Environ. Sci. Technol. 36, 2109–2115.

Brooks, S.P., Gelman, A., 1998. General methods for monitoring convergence of iterative simulations. J. Comput. Graph. Stat. 7, 434–455.

Cheng, V., Arhonditsis, G.B., Brett, M.T., 2010. A revaluation of the lake-phosphorus loading models using a Bayesian hierarchical framework. Ecol. Res. 25, 59–76.

Environment Canada (EC), Ontario Ministry of the Environment (OMOE), 2011. St. Marys River Area of Concern, Canadian Section: Status of Beneficial Use Impairments. Available at http://www.ec.gc.ca/Publications/default.asp?lang=En&xml=06B66472-5C30-4B8B-8149-AC38503ABFF7.

Fielder, D.G., Godby, N., Bowen, A., O'Connor, L., Parish, J., Greenwood, S., Chong, S., Wright, G., 2007. Population dynamics of the St. Marys River fish community 1975–2006 (Available online).

French Planning Services Inc. (FPS), 2010. St. Marys River Area of Concern workshop summary of Canadian discussions: updating delisting criteria (Available online).

Gelman, A., Jakulin, A., Pittau, M.G., Su, Y., 2008. A weakly informative default prior distribution for logistic and other regression models. Ann. Appl. Stat. 2, 1360–1383.

Gelman, A., Hill, J., Yajima, M., 2009. Why we (usually) don't have to worry about multiple comparisons. Available at: http://www.stat.columbia.edu/~gelman/research/unpublished/multiple2f.pdf.

Gilks, W.R., Roberts, G.O., Suhu, S.K., 1998. Adaptive Markov Chain Monte Carlo through regeneration. J. Am. Stat. Assoc. 93, 1045–1054.

Gudimov, A., Ramin, M., Labencki, T., Wellen, C., Shelar, M., Shimoda, Y., Boyd, D., Arhonditsis, G.B., 2011. Predicting the response of Hamilton Harbour to the nutrient loading reductions: a modeling analysis of the "ecological unknowns". J. Great Lakes Res. 37, 494–506.

Gudimov, A., O'Connor, E., Dittrich, M., Jarjanazi, H., Palmer, M., Stainsby, E., Winter, J., Young, J., Arhonditsis, G.B., 2012. Continuous Bayesian network for studying the causal links between phosphorus loading and plankton patterns in Lake Simcoe, Ontario, Canada. Environ. Sci. Technol. 46, 7283–7292.

Hayes, M.A., Smith, I.R., Rushmore, T.H., Crane, T.L., Thorn, C., Kocal, T.E., Ferguson, H.W., 1990. Pathogenesis of skin and liver neoplasms in white suckers from industrially polluted areas in Lake Ontario. Sci. Total Environ. 94 (1–2), 105–123.

Hodson, P.V., Munkittrick, K.R., Stevens, R., Colodey, A., 1996. A tier-testing strategy for managing programs of environmental effects monitoring. Can. Water Res. 9, 487–492.

International Joint Commission (IJC), 1998. St. Marys River Area of Concern Status Assessment. Available online at http://www.ijc.org/php/publications/html/stmarys/status.html.

International Joint Commission (IJC), 2012. Delisting targets developed by RAP teams. Available at http://www.ijc.org/rel/boards/annex2/aoc_php/bui_targets.php?bui=Fish%20Tumors%20or%20Other%20Deformities (Accessed Dec. 2012).

Iwanowicz, L.R., Blazer, V.S., Hitt, N.P., McCormick, S.D., DeVault, D.S., Ottinger, C.A., 2012. Histologic, immunologic, and endocrine biomarkers indicate contaminant effects in fishes of the Ashtabula River. Ecotoxicology 21, 165–182.

Johnson, A.K., Law, J.M., Harms, C.A., Levine, J.F., 2007. Multitiered health assessment of Atlantic menhaden in the Pamlico River, North Carolina. J. Aquat. Anim. Health 19, 205–214.

Lauzon, C., Caffo, B., 2009. Easy multiplicity control in equivalence testing using two one-sided tests. Am. Stat. 63, 147–154.

Moerke, A.H., Werner, R.M., 2011. Ecological status of the St. Marys River: foreword. J. Great Lakes Res. 37, 1–4.

North-South Environmental Inc. (NSE), 2003. Lake Superior and St. Marys River AOCs Delisting Criteria and Re-evaluation of BUIs. Available from http://www.lssu.edu/bpac/wp-content/uploads/2011/08/Lake-Superior-and-St.-Marys-River-AOCs-Delisting-Criteria-and-ReEvaluation-of-BUIs-2003.pdf.

Pinkney, A.E., Harshbarger, J.C., May, E.B., Melancon, M.J., 2001. Tumor prevalence and biomarkers of exposure in brown bullheads (*Ameiurus nebulosus*) from the tidal Potomac River, USA, watershed. Environ. Toxicol. Chem. 20, 1196–1205.

Pinkney, A.E., Harshbarger, J.C., May, E.B., Melancon, M.J., 2004. Tumor prevalence and biomarkers of exposure in brown bullhead (*Ameiurus nebulosus*) from Back River, Furnace Creek, and Tuckahoe River, Maryland. Arch. Environ. Contam. Toxicol. 46, 492–501.

Pinkney, A.E., Harshbarger, J.C., Rutter, M.A., 2009. Tumors in brown bullheads in the Chesapeake Bay Watershed: analysis of survey data from 1992 through 2006. J. Aquat. Anim. Health 21, 71–81.

Pratt, T., O'Connor, L.M., 2011. An assessment of the health and historical changes of the nearshore fish community of the St. Marys River. J. Great Lakes Res. 37, 61–69.

Rafferty, S., 2003a. Fish Tumors Related to Great Lakes Areas of Concern Conference Proceedings (Available online).

Rafferty, S., 2003b. Second Fish Tumors Related to Great Lakes Areas of Concern Conference Proceedings (Available online).

Rafferty, S., Grazio, J., 2006. Field manual for assessing internal and external anomalies in brown bullhead (*Ameiurus nebulosus*). Pennsylvania Sea Grant. (29 pp. http://pserie.psu.edu/seagrant/publications/technicaldocs/BullheadFieldManual.pdf).

Rafferty, S.D., Blazer, V.S., Pinkney, A.E., Grazio, J.L., Obert, E.C., Boughton, L., 2009. A historical perspective on the "fish tumors or other deformities" beneficial use impairment at Great Lakes Areas of Concern. J. Great Lakes Res. 35, 496–506.

Reckhow, K.H., Arhonditsis, G.B., Kenney, M.A., Hauser, L., Tribo, J., Wu, C., Elcock, K.J., Steinberg, L.J., Stow, C.A., McBride, S.J., 2005. A predictive approach to nutrient criteria. Environ. Sci. Technol. 39 (9), 2913–2919.

Ripley, M.P., Arbic, B., Zimmerman, G., 2011. Environmental history of the St. Marys River. J. Great Lakes Res. 37, 5–11.

Rutter, M.A., 2010. A statistical approach for establishing tumor incidence delisting criteria in areas of concern: a case study. J. Great Lakes Res. 36, 646–655.

Schaeffer, J.S., Fielder, D.G., Godby, N., Bowen, A., O'Connor, L., Parrish, J., Greenwood, S., Chong, S., Wright, G., 2011. Long-term trends in the St. Marys River open water fish community. J. Great Lakes Res. 37, 70–79.

Spiegelhalter, D.J., Best, N.G., Carlin, B.R., van der Linde, A., 2002. Bayesian measures of model complexity and fit. J. Royal Stat. Soc. Ser. B-Statistical Methodology 64, 583–616.

Spiegelhalter, D., Thomas, A., Best, N., Lunn, D., 2003. WinBUGS User Manual, Version 1.4. Available from http://www.mrc-bsu.cam.ac.uk/bugs/winbugs/manual14.pdf (accessed May 2012).

St. Marys River RAP, 1992. Stage I Report. Available at http://www.lssu.edu/bpac/Materials/St._Marys_River_RAP_Stage1.pdf.

Van der Oost, R., Beyer, J., Vermeulen, N.P.E., 2003. Fish bioaccumulation and biomarkers in environmental risk assessment: a review. Environ. Toxicol. Pharmacol. 13, 57–149.

Vogelbein, W.K., Fournie, J.W., Van Veld, P.A., Huggett, R.J., 1990. Hepatic neoplasms in the mummichog *Fundulus heteroclitus* from a creosote contaminated site. Cancer Res. 50, 5978–5986.

Willis, R.A., 1952. The Spread of Tumors in the Human Body. Butterworth and Co., London.

Zhang, W., Arhonditsis, G.B., 2008. Predicting the frequency of water quality standard violations using Bayesian calibration of eutrophication models. J. Great Lakes Res. 34, 698–720.

A BAYESIAN METHODOLOGICAL FRAMEWORK FOR SETTING FISH TUMOUR OCCURRENCE DELISTING CRITERIA: A CASE STUDY IN ST. MARYS RIVER AREA OF CONCERN

Maryam Mahmood, E. Agnes Blukacz-Richards, Paul C. Baumann, Mark McMaster, Monir Hossain, George B. Arhonditsis

[Electronic Supplementary Material]

List of Supplementary Tables

Table S1: Summary statistics for white sucker physical characteristics across exposed and reference sampling sites in St. Marys River.

	Exposed sites			**Reference site**		
Number of samples	**139** *(41 from Partidge Point, 98 from Bellevue Marina)*			**100** *(all from Batchawana Bay)*		
Age of fish *(mean, SD, median)*	11.01	4.11	10.00	9.81	3.09	10.00
Average female age		11.72			10.16	
Average male age		9.76			9.33	
Fork length (cm) *(mean, SD, median)*	43.64	3.77	43.80	44.30	3.86	44.15
Total weight (g) *(mean, SD, median)*	1188	291	1190	1237	298	1200
Gonad weight (g) *(mean, SD, median)*	63.05	23.74	61.59	77.02	31.28	77.24
Liver weight (g) *(mean, SD, median)*	18.74	8.04	18.02	17.20	7.30	16.08

Table S2: Summary of parameter posteriors for the most parsimonious models.

	Model version	Parameters							
		α		β_0		β_1		β_2	
		mean	*SD*	*mean*	*SD*	*mean*	*SD*	*mean*	*SD*
	MODEL ONE								
EXPOSED	Cholangioma *(Age + GW)*	*N/A*		-6.562	1.697	2.409	0.876	-1.061	0.494
EXPOSED	Cholangiocarcinoma *(Age + LW)*			0.612	0.601	0.440	0.890	0.536	0.612
EXPOSED	Bile duct hyperplasia *(Age + FL)*			-3.840	0.677	0.526	0.569	0.939	0.794
EXPOSED	Total neoplasms *(Age + FL)*			0.366	0.897	0.411	0.040	0.490	0.366
REF.	Bile duct hyperplasia *(Age + LW)*			-46.24	18.90	5.804	2.720	19.59	8.192
REF.	Total preneoplasms *(Age + LW)*			-2.235	0.357	0.475	0.340	0.226	0.394
	MODEL TWO								
EXPOSED	Cholangioma *(Age + GW)*	2.343	0.327	-2.867	0.987	1.229	0.613	-0.249	0.372
EXPOSED	Cholangiocarcinoma *(Age + LW)*	2.586	0.474	-1.811	0.815	-0.136	0.480	1.841	1.067
EXPOSED	Bile duct hyperplasia *(Age + LW)*	2.665	0.516	-1.914	0.865	1.950	1.218	-0.168	1.287
EXPOSED	Total neoplasms *(Age + FL)*	2.225	0.218	-0.540	0.325	0.254	0.334	0.075	0.442
REF.	Bile duct hyperplasia *(Age + LW)*	2.530	0.502	-9.722	5.138	1.300	0.955	3.960	2.466
REF.	Total preneoplasms *(Age + LW)*	2.229	0.211	-0.574	0.368	0.224	0.433	-0.029	0.428
	MODEL THREE								
EXPOSED	Cholangioma *(Age + GW)*	3.144	0.805	-2.796	1.230	1.980	0.658	-0.835	0.367
EXPOSED	Cholangiocarcinoma *(Age + FL)*	2.667	0.581	-0.983	0.503	0.817	0.536	0.205	0.647
EXPOSED	Bile duct hyperplasia *(Age + FL)*	4.026	0.736	-1.049	0.684	0.891	0.636	0.693	0.862
EXPOSED	Total neoplasms *(Age + FL)*	2.738	0.598	-0.154	0.354	0.917	0.406	-0.105	0.451
REF.	Bile duct hyperplasia *(Age + LW)*	3.540	0.867	-20.13	11.41	3.067	1.767	10.21	5.105
REF.	Total preneoplasms *(Age + LW)*	3.457	0.752	0.376	0.531	0.529	0.352	0.312	0.441

Table S3: Spearman rank correlation coefficients for white sucker physical characteristics in the St. Marys River exposed sites (Bellevue Marina and Partridge Point) and reference site (Batchawana Bay). All correlations were significant at the 5% level of significance.

Exposed sites					
	Age	**Fork length**	**Total weight**	**Gonad weight**	**Liver weight**
Age	1.000	0.798	0.674	0.372	0.599
Fork length	0.798	1.000	0.855	0.565	0.768
Total weight	0.674	0.855	1.000	0.724	0.846
Gonad weight	0.372	0.565	0.724	1.000	0.632
Liver weight	0.599	0.768	0.846	0.632	1.000
Reference site					
Age	1.000	0.833	0.782	0.581	0.557
Fork length	0.833	1.000	0.955	0.726	0.741
Total weight	0.782	0.955	1.000	0.822	0.780
Gonad weight	0.581	0.726	0.822	1.000	0.571
Liver weight	0.557	0.741	0.780	0.571	1.000

Table S4: Summary of the posteriors from the comparative exercise between exposed and reference sites using the hierarchical configuration of the Bernoulli model.

Neoplasms						Preneoplasms					
Exposed			Reference			Exposed			Reference		
	Mean	*SD*		*Mean*	*SD*		*Mean*	*SD*		*Mean*	*SD*
β_0	-2.589	0.368	β_0	-3.320	0.585	β_0	-1.647	0.236	β_0	-2.066	0.332
β_{age}	0.653	0.349	β_{age}	0.078	0.686	β_{age}	0.269	0.223	β_{age}	0.502	0.348
$\beta_{flength}$	0.242	0.445	$\beta_{flength}$	0.443	0.589	$\beta_{lvweight}$	0.025	0.251	$\beta_{lvweight}$	0.192	0.334
Frequency int.		*upper*	*lower*			***Frequency int.***		*upper*	*lower*		
Difference*		8.59%	-2.64%			Difference		12.22%	-3.43%		
Tolerance level**		10.66%	-10.76%			Tolerance level		12.68%	-12.81%		

* Refers to the difference of the predicted tumour incidence between exposed and reference sites.

** The tolerance level was determined by comparing the exposed site to itself, using two independent MCMC samples from the corresponding posterior distribution of the predicted tumour incidence. The bound of this interval that is greatest in absolute value can be viewed as the tolerance level required for two sites with sampling designs similar to the exposed one to exhibit equivalence if the true tumor incidence at the sites were identical. To allow sites with similar, but not exact, tumor incidences to demonstrate evidence of equivalence, 5% was added to the initial tolerance level estimate.

WinBUGS codes (Total neoplasms)

Bernoulli model

```
model {

          for (i in 1 : N) {
            Tumor[i]~dbern(p[i])
            logit(p[i])<-pmu[i]
            pmu[i]<-beta0+beta1*((Age[i]-Age_mean)/Age_sd)+beta2*((Fork_length[i]-
                    Fork_length_mean)/Fork_length_sd)
                          }
         Age_mean<-mean(Age[])
         Age_sd<-sd(Age[])
         Fork_length_mean<-mean(Fork_length[])
         Fork_length_sd<-sd(Fork_length[])

          beta0 ~ dnorm(0, 0.001)
          beta1 ~ dnorm(0, 0.001)
          beta2 ~ dnorm(0, 0.001)

        }
```

list(N = 139,

Tumor =
c(0,0,0,0,0,0,0,0,1,1,0,1,0,0,0,0,0,0,0,0,0,0,0,0,0,0,1,0,0,0,0,0,0,0,0,0,0,0,0,0,0,0,0,0,1,0,0,0,0,0,0,0,0,0,1,1,1,0,0,0,0,1,0,0,0,0,
0,1,0,0,0,0,0,0,0,1,0,0,0,0,0,0,0,0,0,0,0,0,0,1,0,0,0,0,0,0,0,0,0,0,0,1,0,0,0,0,0,0,0,0,0,0,0,0,0,0,0,0,0,0,0,0,0,0,0,0,0,1,0,0,0,0,
0,0,0,0,0,0),

Age =
c(8,12,12,9,8,17,6,13,15,19,7,8,9,16,12,15,7,11,9,10,10,9,8,13,7,18,7,8,10,7,7,7,6,12,14,9,7,7,8,16,5,7,14,16,9,8,6,8,13,20,16
,8,12,15,6,14,23,7,11,8,17,9,7,15,10,9,7,16,11,10,13,10,8,7,8,16,12,12,15,6,15,10,11,10,7,18,12,15,16,11,8,9,9,7,11,12,6,6,1
7,13,5,13,11,7,11,19,17,15,10,8,5,17,5,7,15,13,6,12,8,9,7,6,11,14,5,6,15,14,21,12,13,10,15,19,10,17,19,18,6),

Fork_length =
c(3.728100167,3.899950424,3.828641396,3.795489189,3.706228092,3.850147602,3.706228092,3.914021008,3.817712326,
3.929862924,3.73289634,3.740047741,3.83081295,3.887730313,3.797733859,3.742420221,3.772760938,3.788724789,3.79
7733859,3.864931398,3.768152635,3.786459782,3.811097087,3.804437795,3.660994251,3.889777396,3.701301974,3.688
879454,3.817932082,3.678829118,3.691376334,3.706228092,3.713572067,3.839452313,3.891820298,3.758871826,3.6913
76334,3.686376324,3.7208625,3.779633817,3.597312261,3.756538103,3.864931398,3.703768067,3.698829785,3.7658404
95,3.610917913,3.795489189,3.841600541,3.862832761,3.90197267,3.758871826,3.871201011,3.850147602,3.698829785,
3.90197267,3.879499814,3.703768067,3.850147602,3.761200116,3.90197267,3.848017675,3.725693427,3.871201011,3.80
666249,3.747148362,3.761200116,3.850147602,3.828641396,3.784189634,3.835141961,3.737669618,3.713572067,3.7135
72067,3.772760938,3.860729711,3.772760938,3.747148362,3.772760938,3.681351188,3.83081295,3.777348102,3.784189
634,3.740047741,3.686376324,3.867025639,3.837299459,3.793239469,3.843744165,3.813307032,3.871201011,3.7424202
21,3.793239469,3.758871826,3.761200116,3.777348102,3.632309103,3.583518938,3.864931398,3.725693427,3.51154543
9,3.786459782,3.763522997,3.742420221,3.850147602,3.790984677,3.879499814,3.804437795,3.793239469,3.660994251,
3.549617387,3.860729711,3.532225644,3.645449896,3.819907717,3.742420221,3.589059119,3.845883203,3.723280881,3.
751854253,3.666122467,3.583518938,3.713572067,3.73289634,3.538056564,3.62700405,3.813307032,3.841600541,3.903
990834,3.713572067,3.826465117,3.78191432,3.852273001,3.797733859,3.839452313,3.925925911,3.912023005,3.86283
2761,3.62700405))

#Initial Conditions 1
list(beta0 = 1, beta1 = 1, beta2 = 1)

#Initial Conditions 2
list(beta0 = 0.5, beta1 = 0.5, beta2 = 0.5)

#Initial Conditions 3
list(beta0 = 1.2, beta1 = 1.2, beta2 = 1.2)

Zero-Inflated Poisson model

```
model {

        for (i in 1 : N) {
          Tumor[i] ~ dpois(mu[i])
          mu[i]<-u[i]*(pmu[i])
          u[i]~dbern(p[i])
          #Fork_length_min[i]<-Fork_length[i]-0.1
          #Fork_length_max[i]<-Fork_length[i]+0.1
          #Fork_length_rand[i]~dunif(Fork_length_min[i],Fork_length_max[i])
           p[i]<-exp(-alpha/(Number[i]))
           #log(pmu[i])<-beta0+beta1*((Age[i]-Age_mean)/Age_sd)+beta2*((Fork_length_rand[i]-
                        Fork_length_mean)/Fork_length_sd)
           log(pmu[i])<-beta0+beta1*((Age[i]-Age_mean)/Age_sd)+beta2*((Fork_length[i]-
                        Fork_length_mean)/Fork_length_sd)
                       }
        Age_mean<-mean(Age[])
        Age_sd<-sd(Age[])
        Fork_length_mean<-mean(Fork_length[])
        Fork_length_sd<-sd(Fork_length[])

         alpha ~ dunif(2,5)
         beta0 ~ dnorm(0, 0.001)
         beta1 ~ dnorm(0, 0.001)
         beta2 ~ dnorm(0, 0.001)
        }

list(N =40,
Number=c(3,2,7,4,1,14,4,8,6,1,3,7,1,2,7,2,1,6,2,2,5,4,2,4,2,1,4,1,7,3,1,1,5,6,3,2,2,1,1,1),

Tumor = c(0,0,1,1,0,0,0,1,0,0,0,0,1,0,0,0,0,1,0,0,0,0,0,0,0,0,1,0,1,0,1,0,2,1,1,0,1,0,1,1),

Age = c(5,5,6,6,7,7,7,8,8,8,9,9,9,10,10,10,11,11,11,12,12,12,13,13,13,14,14,15,15,15,16,16,16,17,18,19,19,20,21,23),

Fork_length =
c(3.5,3.6,3.6,3.7,3.6,3.7,3.8,3.7,3.8,3.9,3.7,3.8,3.9,3.7,3.8,3.9,3.7,3.8,3.9,3.7,3.8,3.9,3.7,3.8,3.9,3.7,3.9,3.7,3.8,3.9,3.7,3.8,3.9,
3.9,3.9,3.8,3.9,3.9,3.9,3.9))

**#Initial Conditions 1**
list(beta0 = 0.1, beta1 = 0.1, beta2 = 0.1, alpha=2.1, u =
c(0,0,1,1,0,0,0,1,0,0,0,0,1,0,0,0,0,1,0,0,0,0,0,0,0,0,1,0,1,0,1,0,1,1,1,0,1,0,1,1)),

**#Initial Conditions 2**
list(beta0 = 0.5, beta1 = 0.5, beta2 = 0.5, alpha=2, u =
c(0,0,1,1,0,0,0,1,0,0,0,0,1,0,0,0,0,1,0,0,0,0,0,0,0,0,1,0,1,0,1,0,1,1,1,0,1,0,1,1)),

**#Initial Conditions 3**
```

```
list(beta0 = 0.7, beta1 = 0.7, beta2 = 0.7, alpha=2, u =
c(0,0,1,1,0,0,0,1,0,0,0,0,1,0,0,0,0,1,0,0,0,0,0,0,0,0,1,0,1,0,1,0,1,1,1,0,1,0,1,1))
```

Binomial-Poisson model

```
model {

        for (i in 1 : N) {
          Tumor[i] ~ dbin(p[i],Tumorlatent[i])
          Tumorlatent[i]~dpois(lamda[i])
          p[i]<-exp(-alpha/(Number[i]))
          #Fork_length_min[i]<-Fork_length[i]-0.1
          #Fork_length_max[i]<-Fork_length[i]+0.1
          #Fork_length_rand[i]~dunif(Fork_length_min[i],Fork_length_max[i])
          lamda[i] <-exp(lamdam[i])
          #lamdam[i] <-beta0+beta1*((Age[i]-Age_mean)/Age_sd)+beta2*((Fork_length_rand[i]-
                    Fork_length_mean)/Fork_length_sd)
          lamdam[i] <-beta0+beta1*((Age[i]-Age_mean)/Age_sd)+beta2*((Fork_length[i]-
                    Fork_length_mean)/Fork_length_sd)
                      }
        Age_mean<-mean(Age[])
        Age_sd<-sd(Age[])
        Fork_length_mean<-mean(Fork_length[])
        Fork_length_sd<-sd(Fork_length[])

        alpha ~ dunif(2,5)
        beta0 ~ dnorm(0, 0.001)
        beta1 ~ dnorm(0, 0.001)
        beta2 ~ dnorm(0, 0.001)

        }

list(N =40,
Number=c(3,2,7,4,1,14,4,8,6,1,3,7,1,2,7,2,1,6,2,2,5,4,2,4,2,1,4,1,7,3,1,1,5,6,3,2,2,1,1,1),

Tumor = c(0,0,1,1,0,0,0,1,0,0,0,0,1,0,0,0,0,1,0,0,0,0,0,0,0,0,1,0,1,0,1,0,2,1,1,0,1,0,1,1),

Age = c(5,5,6,6,7,7,7,8,8,8,9,9,9,10,10,10,11,11,11,12,12,12,13,13,13,14,14,15,15,15,16,16,16,17,18,19,19,20,21,23),

Fork_length =
c(3.5,3.6,3.6,3.7,3.6,3.7,3.8,3.7,3.8,3.9,3.7,3.8,3.9,3.7,3.8,3.9,3.7,3.8,3.9,3.7,3.8,3.9,3.7,3.8,3.9,3.7,3.9,3.7,3.8,3.9,3.7,3.8,3.9,
3.9,3.9,3.8,3.9,3.9,3.9,3.9))

#Initial Conditions 1
list(beta0 = 0.1, beta1 = 0.1, beta2 = 0.1 , alpha = 2.1,
Tumorlatent=c(3,2,7,4,1,14,4,8,6,1,3,7,1,2,7,2,1,6,2,2,5,4,2,4,2,1,4,1,7,3,1,1,5,6,3,2,2,1,1,1))

#Initial Conditions 2
list(beta0 = 0.2, beta1 = 0.2, beta2 = 0.2 , alpha = 2,
Tumorlatent=c(3,2,7,4,1,14,4,8,6,1,3,7,1,2,7,2,1,6,2,2,5,4,2,4,2,1,4,1,7,3,1,1,5,6,3,2,2,1,1,1))

#Initial Conditions 3
list(beta0 = 0.6, beta1 = 0.6, beta2 = 0.6 , alpha = 1.5,
Tumorlatent=c(3,2,7,4,1,14,4,8,6,1,3,7,1,2,7,2,1,6,2,2,5,4,2,4,2,1,4,1,7,3,1,1,5,6,3,2,2,1,1,1))
```